Supporting Information

A Novel Cadmium-Containing Porphyrin-Based Metal-Organic Framework Enables Oxidation of Inert C(sp^3)−H Bonds

1. Experimental Section.

Materials and methods

All substrates were used as received from commercial suppliers, unless otherwise stated. Chemicals were purchased from Sigma-Aldrich, Chempur, TCI, or Alfa Aesar. Powder X-ray diffraction (PXRD) using a Bruker D8 Advance X-ray diffractometer (Cu Kα radiation, $\lambda = 1.5418$ Å) in the range of 5-50°(2θ). Scanning electron microscopy (SEM) images were taken using a Field Emission Scanning Electron Microscopy SU8600. Fourier transform infrared spectra (FT-IR) were recorded as KBr pellets on a NEXUS instrument in the range of 500−4000 cm^{-1}. Thermogravimetric analyses (TGA) were performed at a ramp rate of 10°C/min in a nitrogen flow with an SDTQ600 instrument. X-ray photoelectron spectroscopy (XPS) signals were collected on a Thermo ESCALAB Xi+ spectrometer. Liquid UV-vis spectra were performed on a TU-1900 spectrophotometer. Solid UV−vis spectra were obtained using a Hitachi U-4100 UV−vis−NIR spectrophotometer and a white standard of $BaSO_4$ was used as a reference. Fluorescent spectra were recorded on the Edinburgh FLS1000 stable fluorescence spectrometer. Electrochemical experiments were carried out on CHI760E workstation with three-electrode system. Photocurrent responses, and electrochemical impedance spectra were measured on a CHI760E electrochemical workstation. HPLC analysis was performed on a SHIMADZU LC 2030 Plus analyzer using a ZORBAX SB-C18 reversed-phase column (250×4.6mm I. D, s-5μM) and eluted with acetonitrile and water. Electron paramagnetic resonance (EPR) experiments were conducted on a Bruker E500 instrument. The ^1H NMR spectra were recorded by a Bruker AVANCE NEO 500MHz instrument with ^1H NMR chemical shifts of 7.26 ppm for $CDCl_3$ solvent. The light sources are 30 W 365 nm LED.

Preparation

Synthesis of Ligand

(1) Synthesis of compound **TCPPMe**. Firstly, dissolve methyl p-formylbenzoate (7g, 42.6mmol) in propionic acid (200ml), and then add pyrrole (3g, 44.7mmol) dropwise to the above solution. Reflux the mixed solution at 160 ℃ overnight After the reaction mixture was reduced to room temperature, the purple crystal products were obtained by suction filtration and washed with methanol and water. Yield: 50%

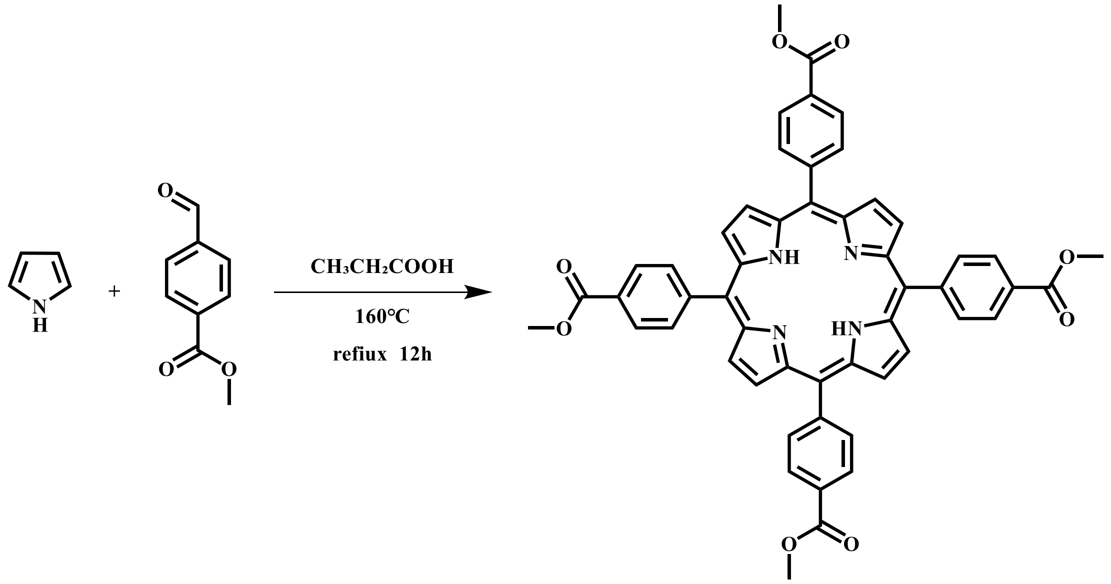

Figure S1. Synthetic procedure for tetramethyl 4,4',4'',4'''-(porphyrin-5,10,15,20-tetrayl) tetrabenzoate (TCPPMe). [S1, S2]

(2) Synthesis of ferric chloride porphyrin complex **Mn-TCPPMe**. TCPPMe (1.5 g, 1.77 mmol) and $MnCl_2•4H_2O$ (5 g, 25.6 mmol) were put into DMF (200 mL) and then heated to reflux for 12 h. The obtained precipitate was obtained by suction filtration and washed twice with water. The remaining solid was dissolved in chloroform and purified using solvent extraction (1 M HCl extraction for 3 times and

water extraction for 2 times). And the quantitative dark brown crystals were obtained by spin evaporation. Yield: 60%.

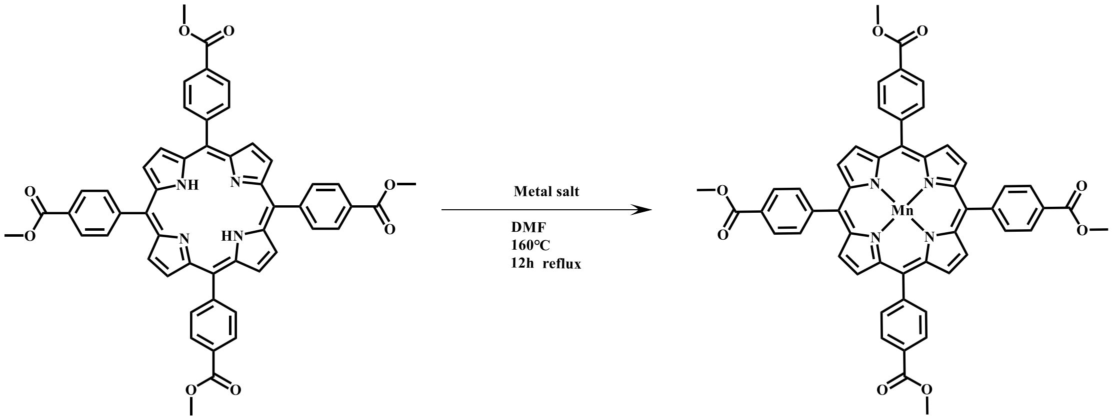

Figure S2. Synthetic procedure for [5,10,15,20-Tetra(4-methoxycarbonylphenyl) porphyrin]-manganese (Mn-TCPPMe). [S1]

(3) Synthesis of **Mn-TCPP**. Mn-TCPPMe (1.5 g,1.67mmol) was stirred with a mixture of THF (50 mL) and MeOH (50 mL), followed by the addition of KOH solution, in which 5.2 g KOH was dissolved in 50 mL water. The mixture was in a reflux state (85℃) for 12 h. After the reaction mixture was reduced to room temperature, THF and MeOH were evaporated. Additional water was added to the resulting aqueous phase, and the mixture was heated until the solid was completely dissolved. The resulting homogeneous solution was then acidified with 1 mol·L^{-1} HCl until the precipitate was no longer formed. The brown solid was obtained by filtering with water and drying in a vacuum. The solid was collected by filtration, washed with water, and dried in vacuum. Yield: 80%.

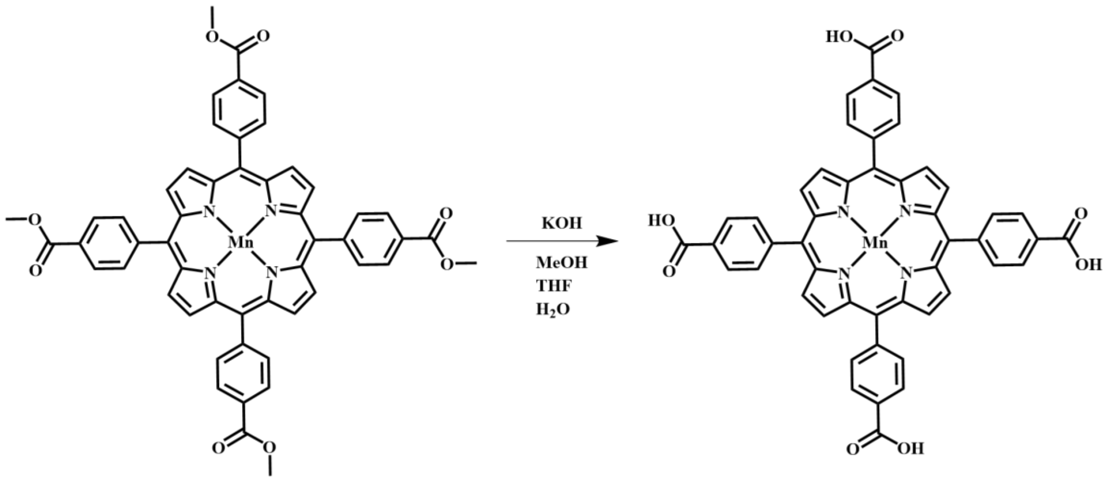

Figure S3. Synthetic procedure for [5,10,15,20-Tetra(4-carboxyphenyl) porphyrinyl]-Mn (Mn-TCPP). [S1]

(4) Synthesis of ferric chloride porphyrin complex **Fe-TCPPMe**. TCPPMe (1.5 g, 1.77 mmol) and $FeCl_2$•$4H_2O$ (5 g, 25.6 mmol) were put into DMF (200 mL) and then heated to reflux for 12 h. The obtained precipitate was obtained by suction filtration and washed twice with water. The remaining solid was dissolved in chloroform and purified using solvent extraction (1 M HCl extraction for 3 times and water extraction for 2 times). And the quantitative dark brown crystals were obtained by spin evaporation. Yield: 65%.

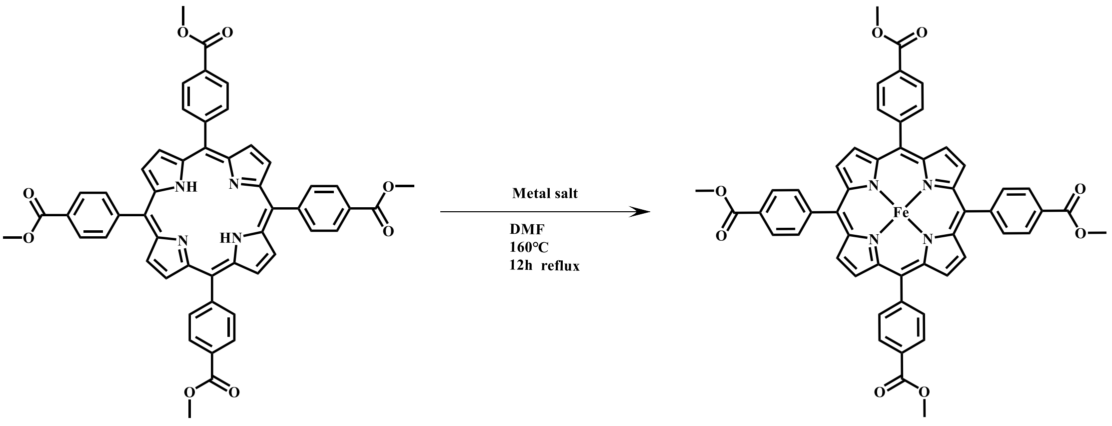

Figure S4. Synthetic procedure for [5,10,15,20-Tetra(4-methoxycarbonylphenyl) porphyrin]-iron (Fe-TCPPMe). [S2]

(5) Synthesis of **Fe-TCPP**. Fe-TCPPMe (1.5 g, 1.67mmol) was stirred with a mixture of THF (50 mL) and MeOH (50mL), followed by the addition of KOH solution, in which 5.2 g KOH was dissolved in 50 mL water. The mixture was in a reflux state (85℃) for 12 h. After the reaction mixture was reduced to room temperature, THF and MeOH were evaporated. Additional water was added to the resulting aqueous phase, and the mixture was heated until the solid was completely dissolved. The resulting homogeneous solution was then acidified with 1 mol·L^{-1} HCl until the precipitate was no longer formed. The brown solid was obtained by filtering with water and drying in a vacuum. The solid was collected by filtration, washed with water, and dried in vacuum. Yield: 82%

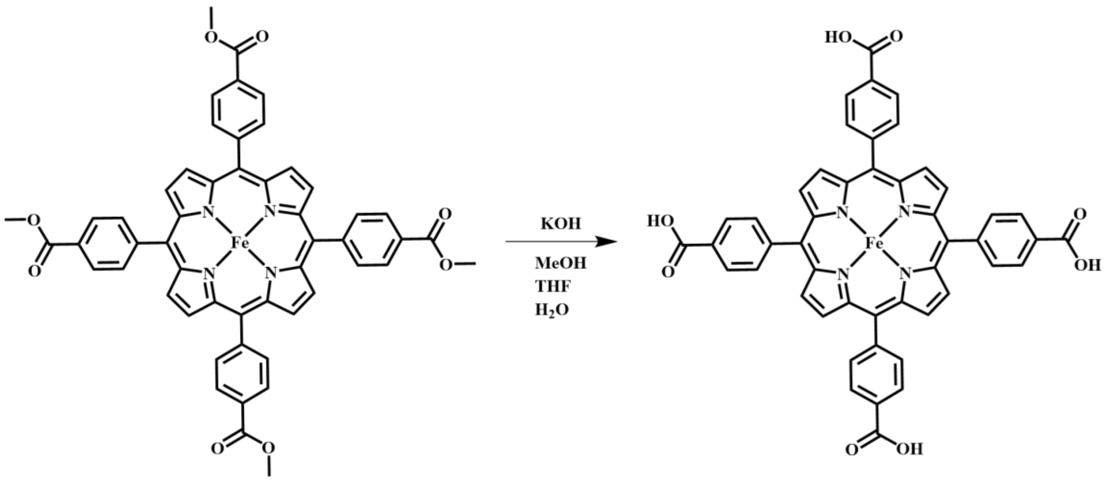

Figure S5. Synthetic procedure for [5,10,15,20-Tetra(4-carboxyphenyl)porphyrinyl]-Fe (Fe-TCPP).

Synthetic procedure of MnTCPP(Cd) and FeTCPP(Cd)

A mixture of $Cd(NO_3)_2{\cdot}4H_2O$ (10 mg, 0.0325 mmol), MnTCPP (10 mg, 0.018 mmol) or FeTCPP (10 mg, 0.018 mmol), and a mixed acid (CF_3COOH: CH_3COOH = 1:1, 0.2 mL) in solution (DMF: CH_3CN: CH_3OH=1:1:1, 3 mL) was sonicated in a 7 mL

Pyrex vial until a homogeneous solution was formed. The solution was then transferred to a Teflon-lined autoclave and heated at 100℃ for 24 h. After the reaction, the system was cooled to room temperature at a rate of 20℃/h. The resulting dark red crystalline product was isolated by filtration, soaked with DMF and acetone for 48 h, and then collected by filtration. Yield of MnTCPP(Cd) and FeTCPP(Cd) was 80% based on the Cd.

General procedure for photocatalytic reactions

All catalytic reactions were carried out under a 365 nm LED. The reaction temperature was maintained at 298K by circulating water through the outer packet of the reactor.

For reactions. 5.0 mg of MnTCPP(Cd) and pyridine 0.02 mmol of hydrochloride was dispersed in 3 mL of CH_3CN, followed by the addition of 0.1 mmol of toluene or 0.1 mmol of toluene derivatives in a 10.0 mL quartz test tube containing a stir bar. The reaction was carried out at ambient temperature for 12h with O_2 bubbling under illumination from a 365 nm LED and magnetic stirring. After the specified time, MnTCPP(Cd) was removed by filtration, and the solvent was evaporated under reduced pressure, the yield was determined by ^{1}H NMR.

Photoelectrochemical Characterization

Photocurrent, electrochemical impedance spectra (EIS), and Mott-Schottky plots of MnTCPP(Cd) and FeTCPP(Cd) were obtained with a three-electrode system employing a photocatalyst-coated FTO working electrode, a Pt plate counter electrode, and an Ag/AgCl reference electrode. All measurements were made in a solution of 1.0 M potassium chloride at room temperature. A 365 nm LED was used as light source. A mixture solution containing 30.0 μL Nafion, and 270.0 μL of Isopropanol was added to the catalyst (5.0 mg). The working electrode is prepared by dripping the mixture onto the surface of the FTO glass about one square centimeter and drying it naturally.

TMB Oxidation Measurement.

Typically, 10 mg of TMB was dissolved in 10 mL of H_2O and 10 mL of HAc / NaAc buffer solution (0.2 M). A total of 100.0 μL of MnTCPP(Cd) or FeTCPP(Cd) aqueous solution (1.0 mg/mL) was then added to the mixture solution with O_2 bubbling under 365 nm LED irradiation. The samples were taken at different time intervals for UV−Vis measurements. In order to verify specific ROS, various scavengers were added to the TMB solution before light irradiation: carotene (2.0 mg), mannite (2.0 mg), catalase (2.0 mg), and superoxide dismutase (SOD, 2.0 mg), respectively.

Fluorescence Lifetime and Fluorescence Quenching Assays.

The solid-state photoluminescence was characterized under 420 nm excitation, with the emission peaks monitored at 650 nm and 720 nm. The fluorescence lifetime at the 650 nm emission was also recorded. A MnTCPP(Cd) DMF solution with a concentration of 1 mg/mL was prepared and centrifuged at 2000 rpm to obtain a supernatant containing a small amount of catalyst. This supernatant was then used for oxygen fluorescence quenching experiments. Prior to oxygen purging, its fluorescence spectrum and lifetime were measured. Subsequently, the changes in the fluorescence emission were recorded after purging with O_2 for 1 minute, and this measurement was repeated every minute for a total of 6 minutes to obtain the quenching profile. Finally, the fluorescence lifetime was measured again after the oxygen purging was complete.

2. Single Crystal X-ray Crystallography

The single crystal MnTCPP(Cd) and FeTCPP(Cd) was directly fixed on a loop and maintained at 240 K during data collection on a Bruker APEX-II CCD diffractometer with Ga-Kα radiation (λ = 1.34139 Å). All data were integrated using SAINT V8.38A, and multi-scan absorption correction was applied with SADABS 2016/2. The structure was solved by direct methods with SHELXT and refined by full-matrix least-squares methods against F^2 using SHELXL. All non-hydrogen atoms were refined with anisotropic displacement parameters. Disordered moieties were refined using bond length restraints and displacement parameter restraints. Crystallographic data for MnTCPP(Cd) and FeTCPP(Cd) have been deposited at the Cambridge Crystallographic Data Centre, CCDC number: **2520103** and **2525830**. The crystallographic data and structure refinement parameters are shown in Table S1.

Table S1. Crystal data and structure refinements.

Compound	**MnTCPP(Cd)**	**FeTCPP(Cd)**
Empirical formula	$C_{48}H_{27.20}CdClMnN_4O_{9.60}$	$C_{100}H_{60}Cd_2Fe_2N_8O_{20}$
Formula weight	1016.33	2030.06
Temperature/K	170.00	170.00
Crystal system	tetragonal	tetragonal
Space group	$P4_32_12$(96)	$P4_12_12$(92)
a/Å	17.0074(7)	17.0110(6)
b/Å	17.0074(7)	17.0110(6)
c/Å	17.4421(9)	17.3513(9)
α/°	90	90
β/°	90	90
γ/°	90	90
Volume/Å^3	5045.2(5)	5021.0(4)
Z	4	2
ρ_{calc}/g·cm^{-3}	1.338	1.343
μ/mm^{-1}	4.373	4.275
F(000)	2040	2048
Crystal size/mm^3	0.38×0.31×0.16	0.24×0.18×0.16
Radiation	GaK$_\alpha$ (λ=1.34139 Å)	GaK$_\alpha$ (λ=1.34139 Å)
2 theta range for data collection/°	6.31 to 121.46 (0.77 Å)	9.96 to 121.33 (0.77 Å)
Index ranges	$-22 \le h \le 20$, $-21 \le k \le 22$, $-22 \le l \le 22$	$-22 \le h \le 18$, $-21 \le k \le 22$, $-22 \le l \le 22$
Reflections collected	89853	71761
Independent reflections	5813, R_{int} = 0.0803, R_{sigma} = 0.0433	5567, R_{int} = 0.0701, R_{sigma} = 0.0391
Data/restraints/parameters	5813/103/297	5567/3/295
Goodness-of-fit on F^2	1.085	1.061
Final R indexes [I>=2σ (I)]	R_1 = 0.0764, wR_2 = 0.2352	R_1 = 0.1070, wR_2 = 0.2857
Final R indexes [all data]	R_1 = 0.0837, wR_2 = 0.2448	R_1 = 0.1131, wR_2 = 0.2938
Largest diff. peak/hole / e Å^{-3}	1.09/−0.69	1.20/−1.42
CCDC number	2520103	2525830

3. Characterizations of Catalysts

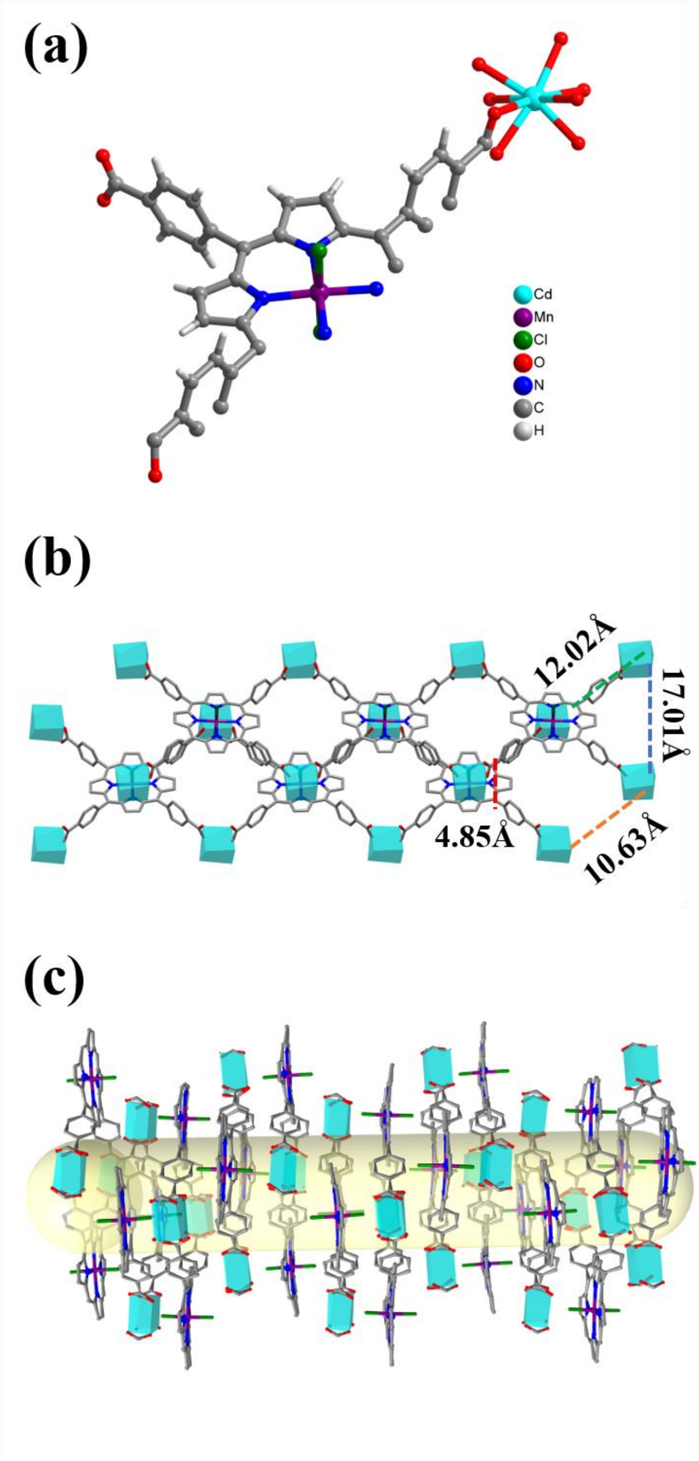

Figure S6. (a) Coordinate environment diagram of the MnTCPP(Cd) asymmetric unit; (b) Hierarchical structure view of MnTCPP(Cd); (c) The three-dimensional packing mode and the intermolecular distance between manganese porphyrins of MnTCPP(Cd).

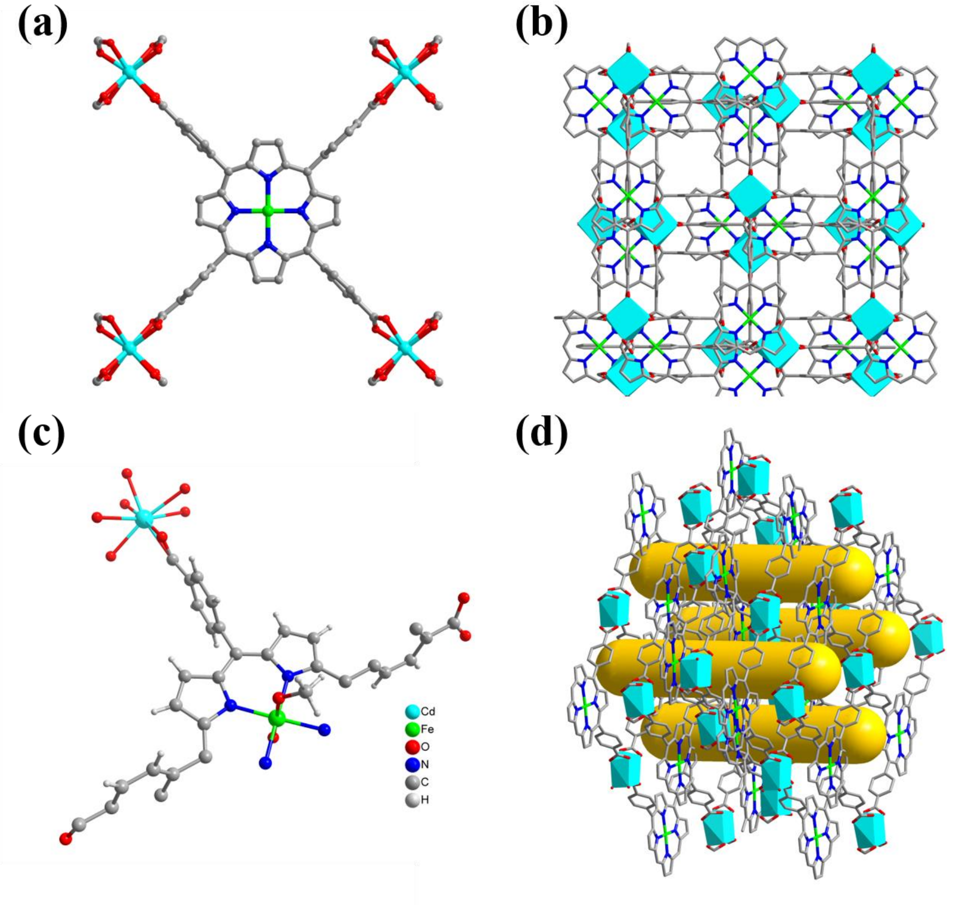

Figure S7. (a) Schematic diagram of ligand bonding in FeTCPP(Cd); (b) Structural view of FeTCPP(Cd) observed along the C-axis direction; (c) Coordinate environment diagram of the FeTCPP(Cd) asymmetric unit; (d) The three-dimensional packing mode and the intermolecular distance between iron porphyrins of FeTCPP(Cd).

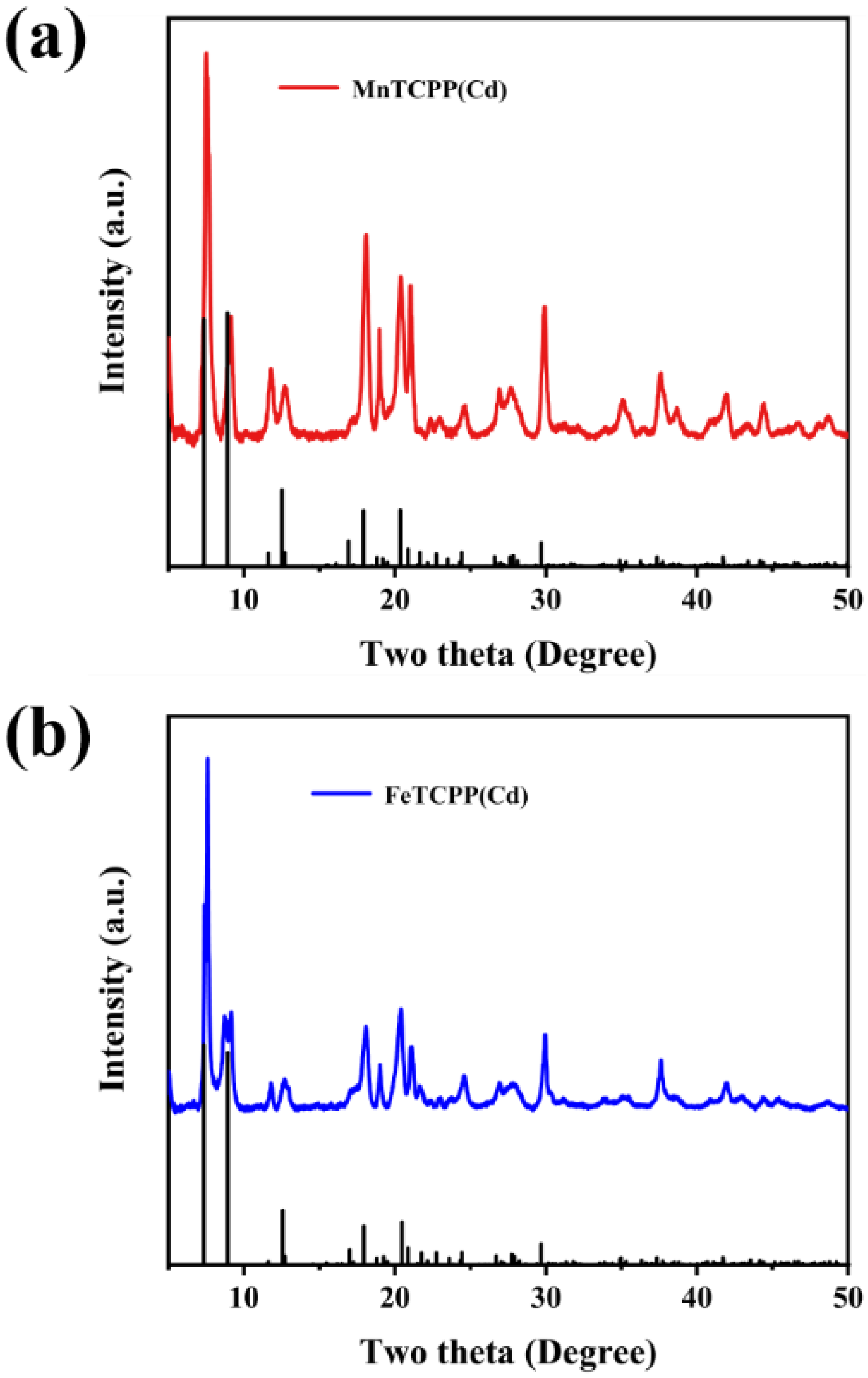

Figure S8. (a) X-ray diffraction patterns of MnTCPP(Cd) powder: single crystal simulation (black), experimental results (red); (b) X-ray diffraction patterns of FeTCPP(Cd) powder: single crystal simulation (black), experimental results (blue)

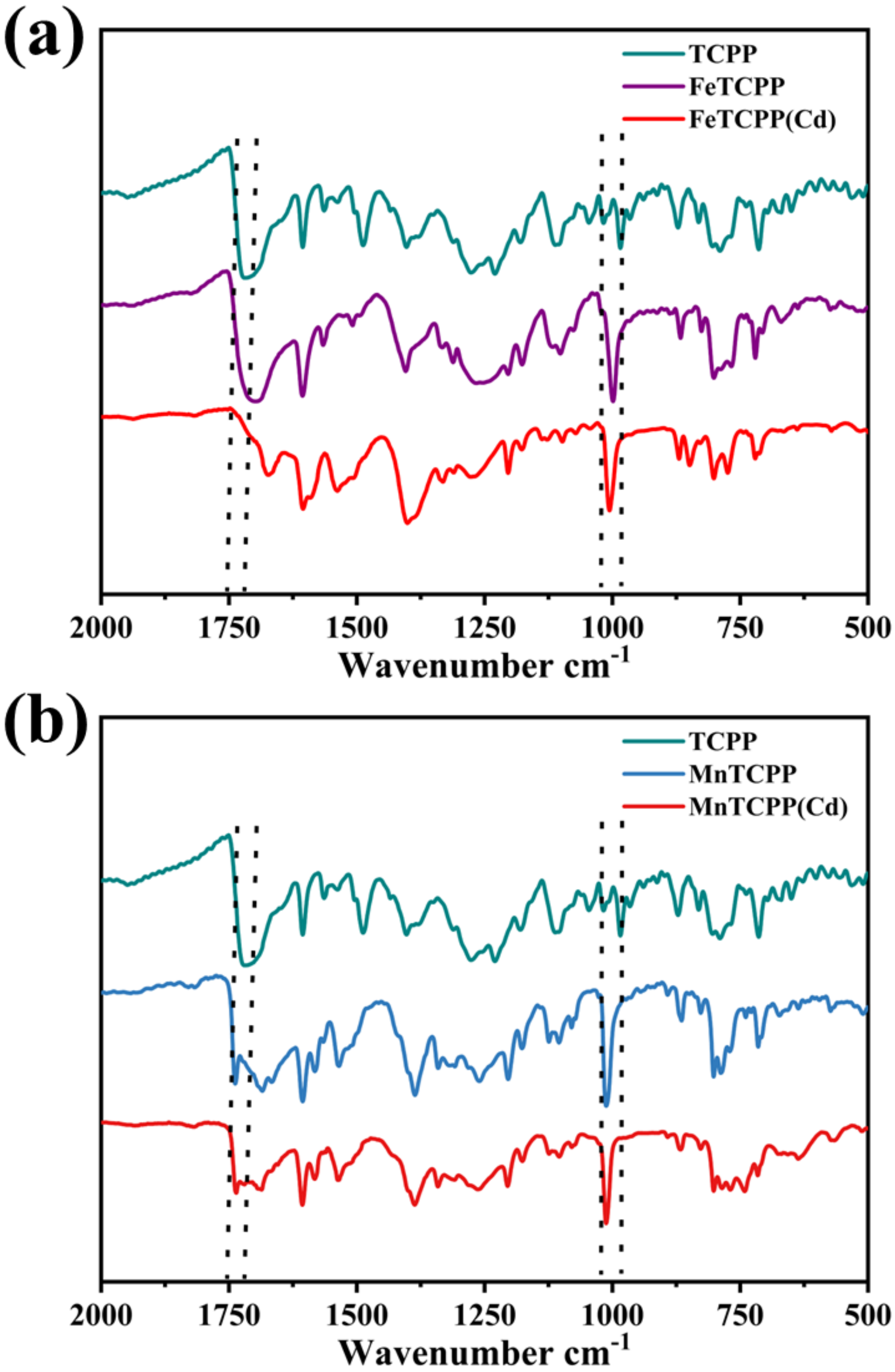

Figure S9. (a) Fourier-transform infrared (FT-IR) spectroscopy of TCPP, FeTCPP, FeTCPP(Cd); (b) Fourier-transform infrared (FT-IR) spectroscopy of TCPP, MnTCPP, MnTCPP(Cd).

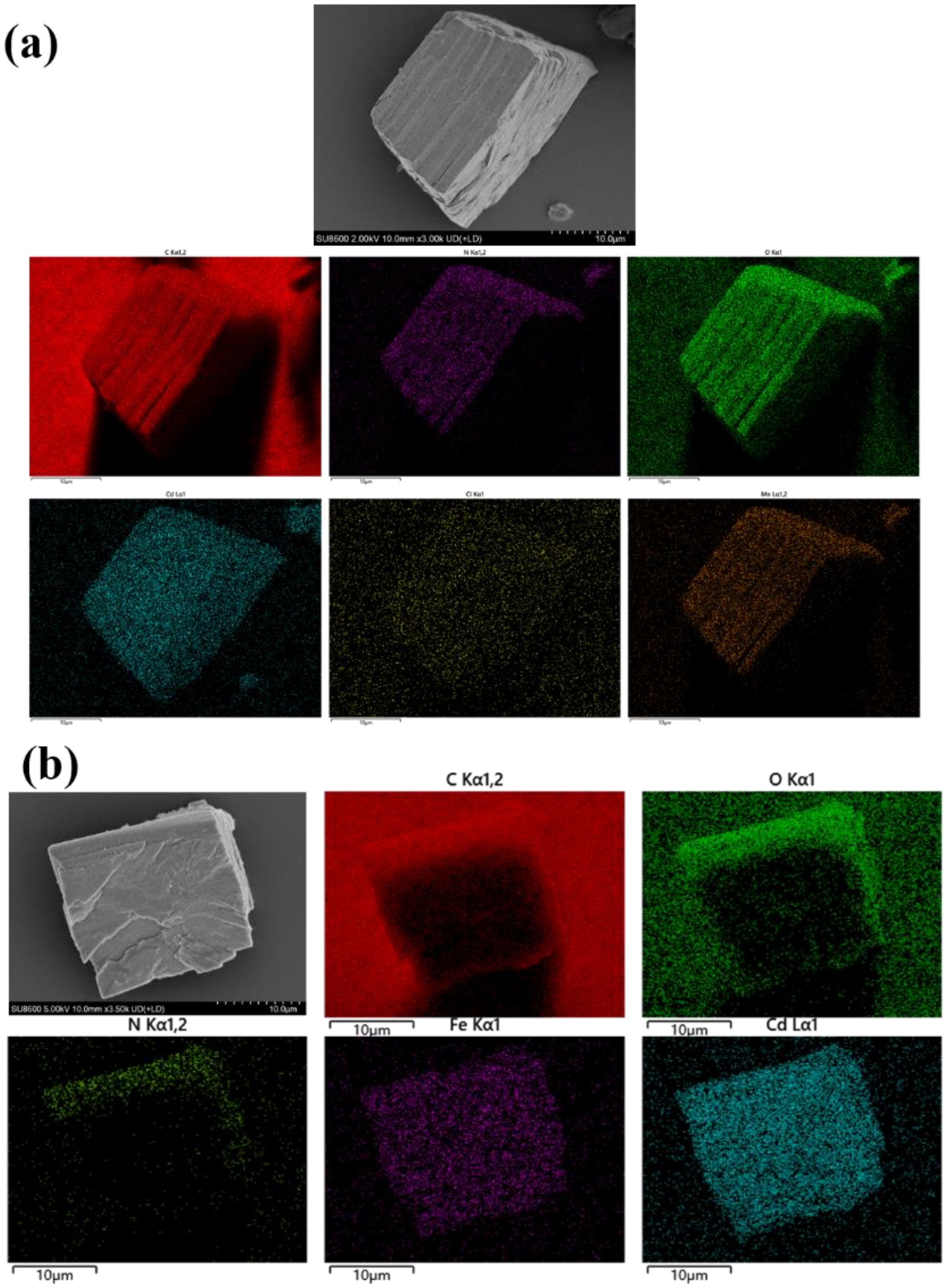

Figure S10. (a) Elemental maps of MnTCPP(Cd) by EDS.; (b) Elemental maps of FeTCPP(Cd) by EDS.

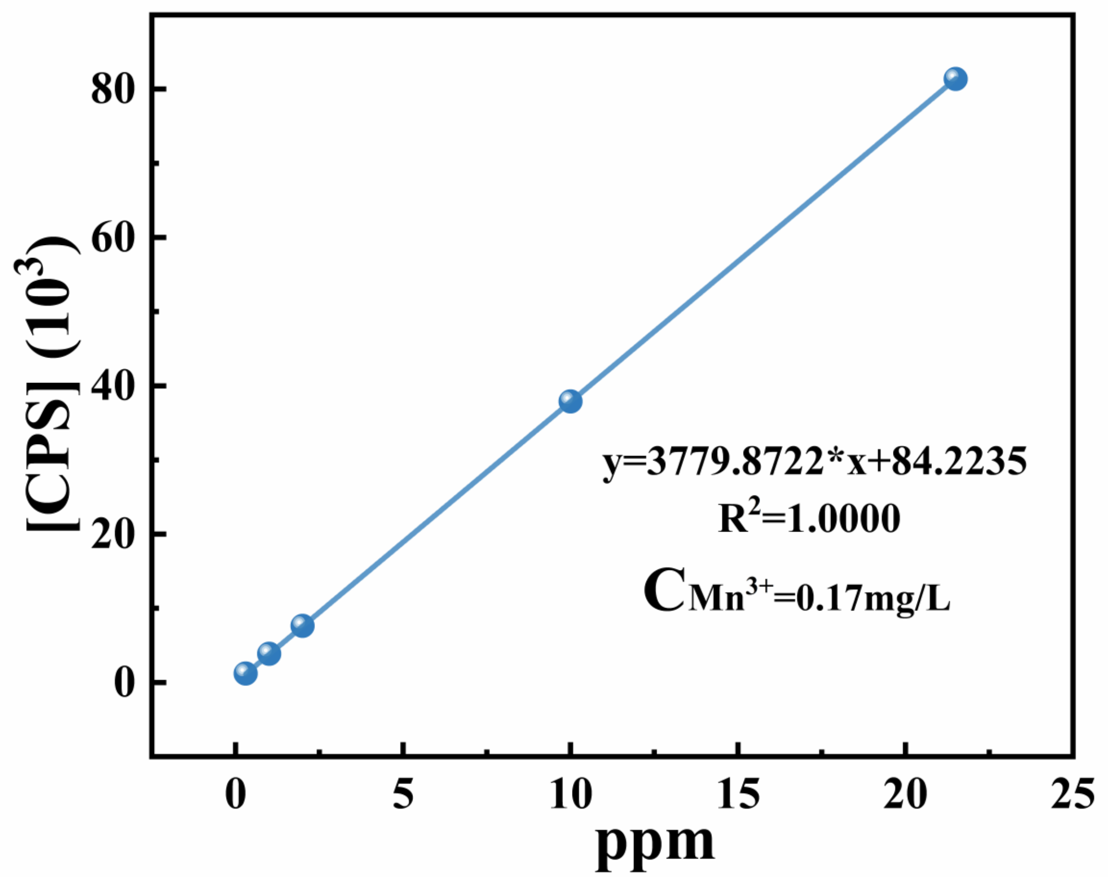

Figure S11. ICP-MS calibration curve for manganese ions and the content of Mn^{3+} in the mother liquor.

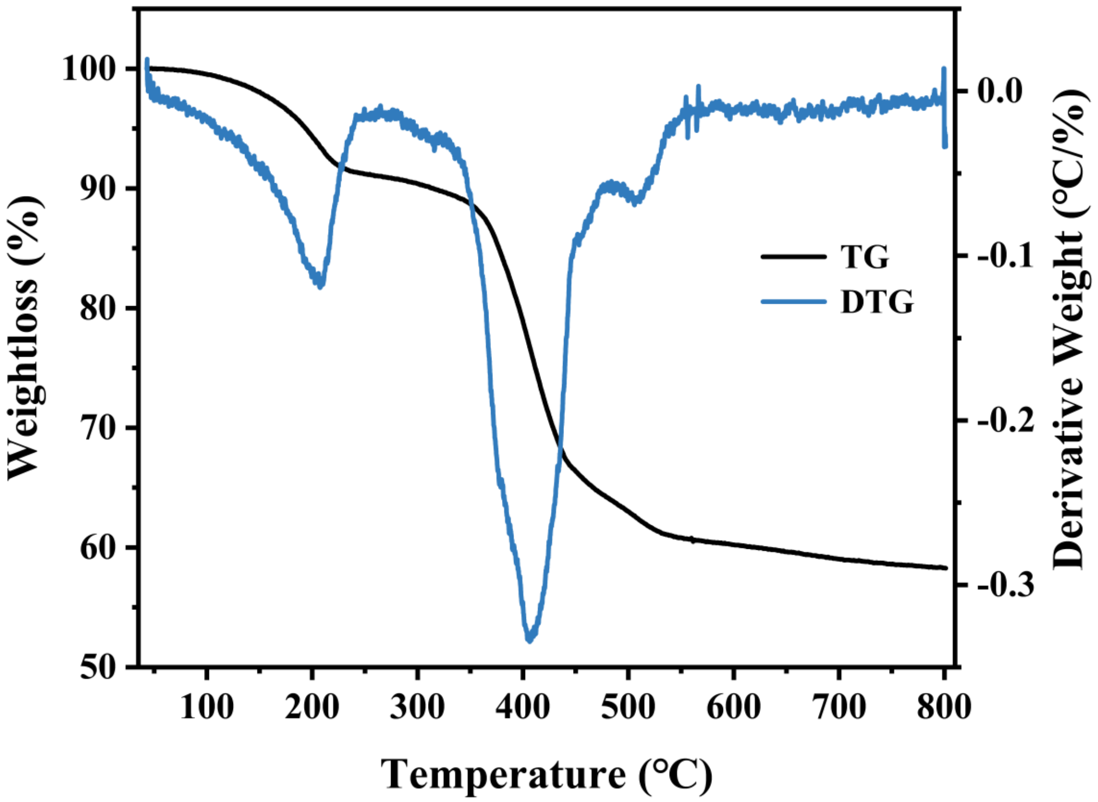

Figure S12. Thermogravimetric (TGA) figure of MnTCPP(Cd) with heating rates of 10℃ /min.

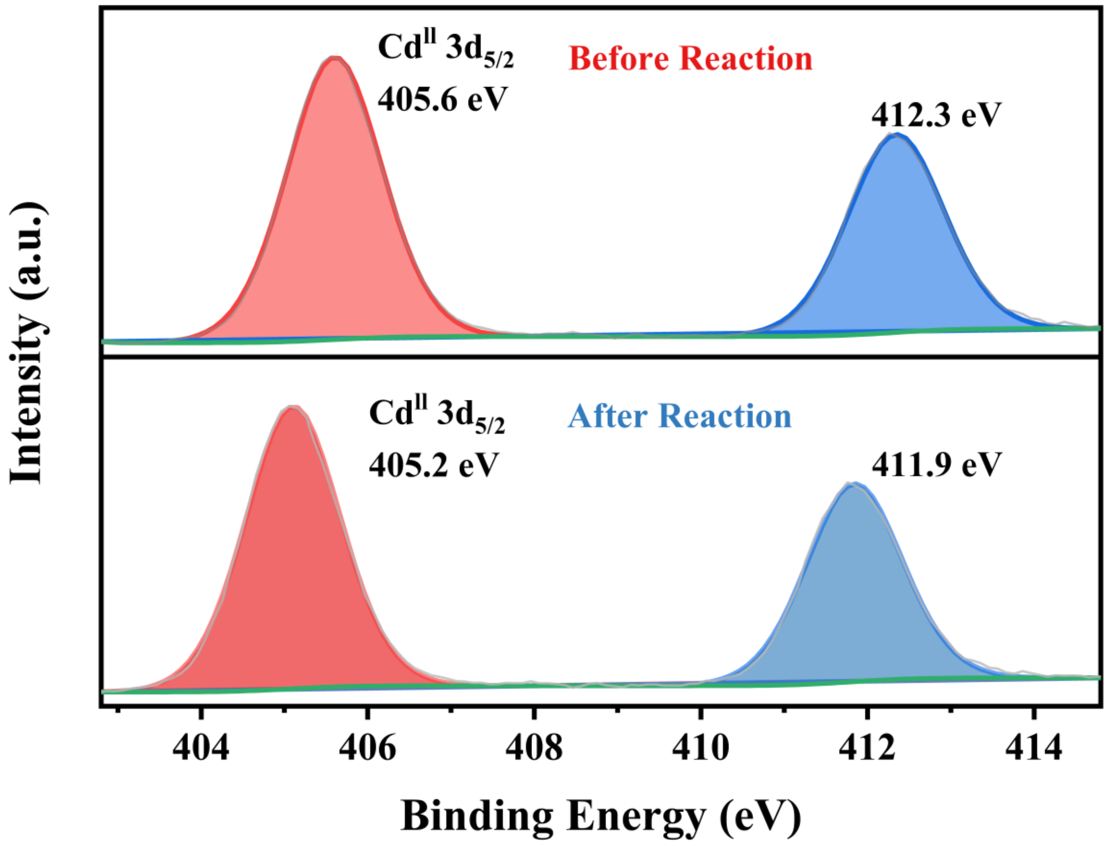

Figure S13. High-resolution Cd 3d XPS spectra of MnTCPP(Cd) and post-reaction samples.

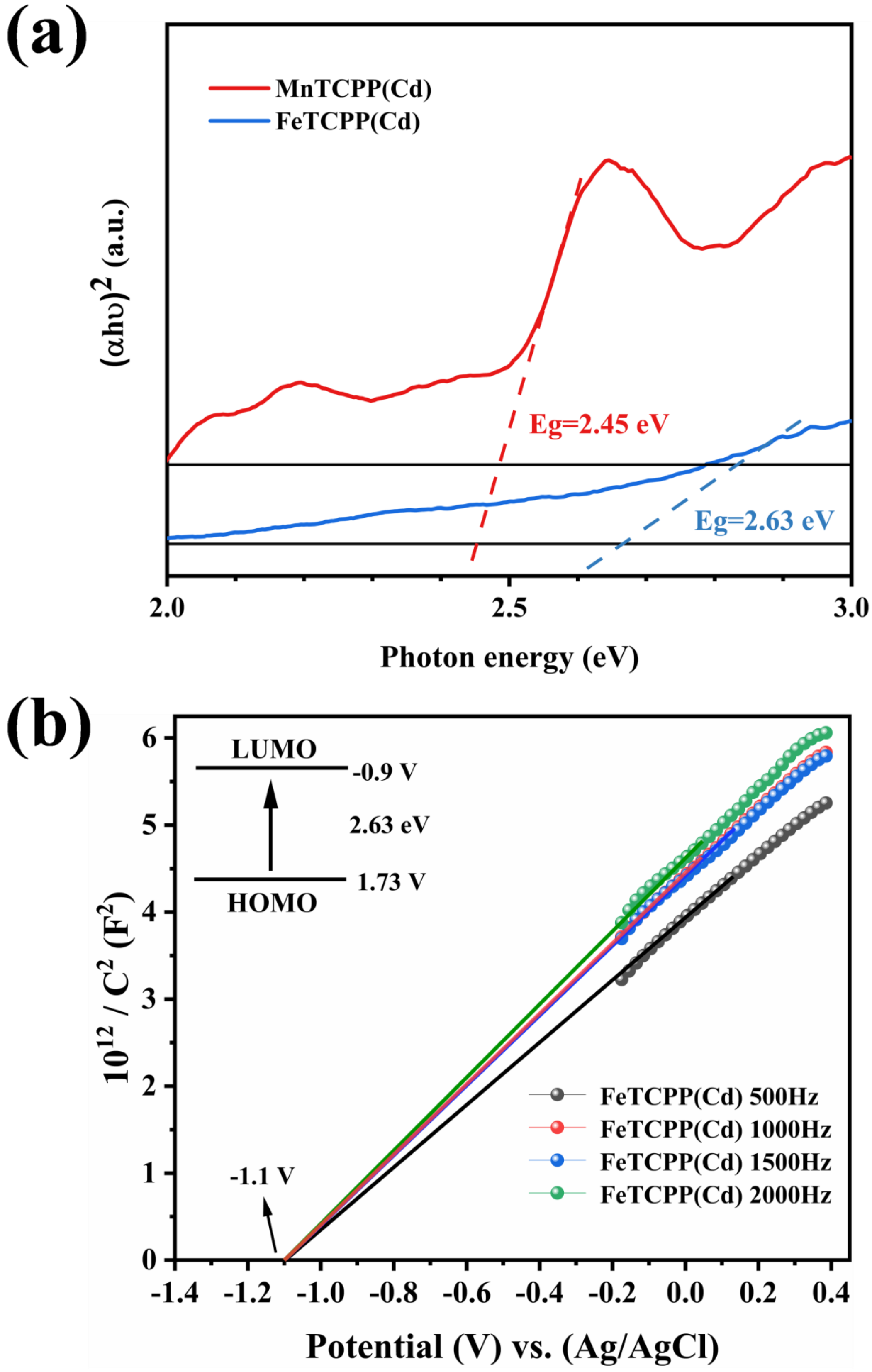

Figure S14. (a) Tauc plots calculate the bandgap of MnTCPP(Cd) and FeTCPP(Cd); (b) Mott–Schottky plots for FeTCPP(Cd).

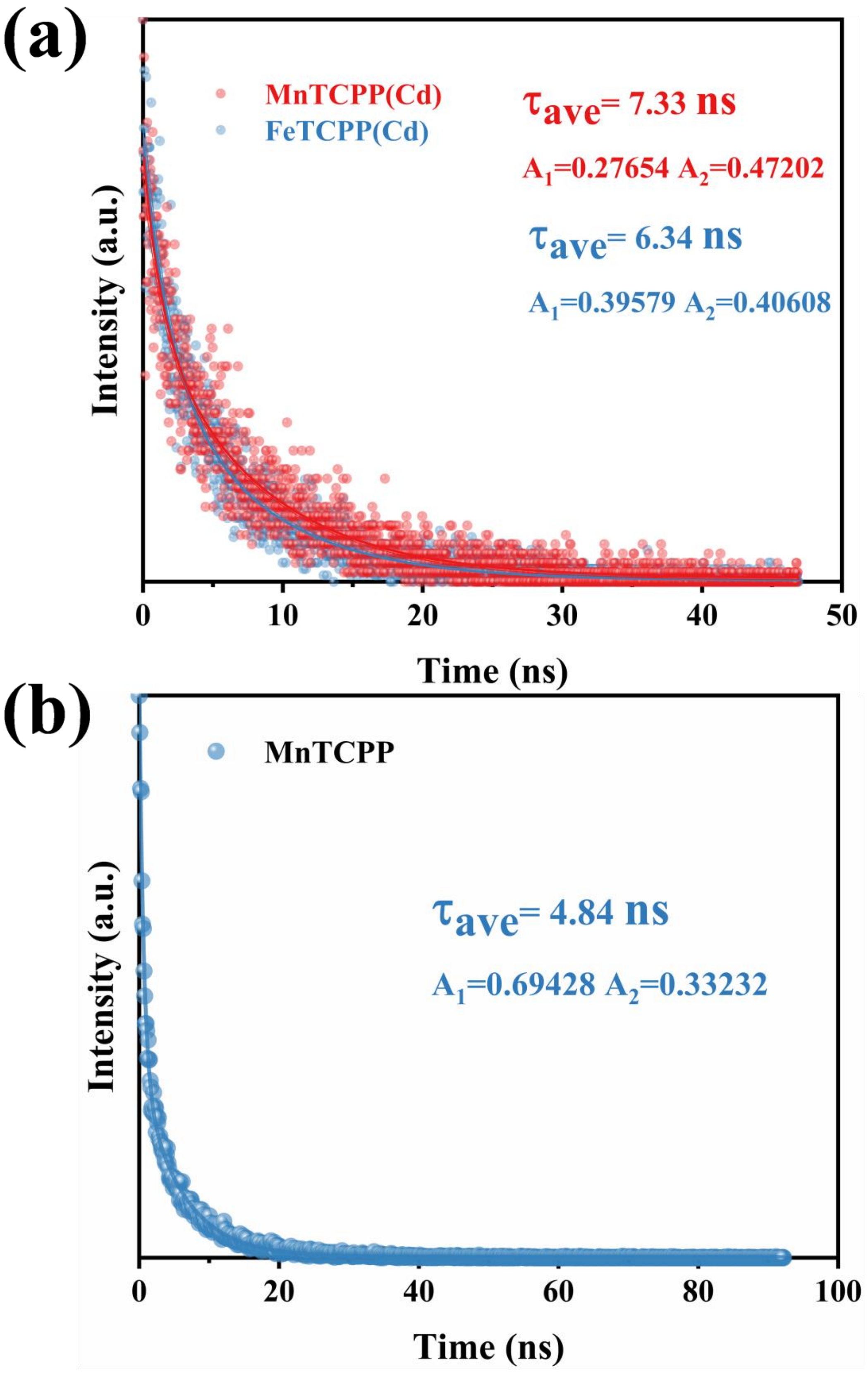

Figure S15. (a) Solid-state fluorescence lifetime of MnTCPP(Cd) and FeTCPP(Cd); (b) Solid-state fluorescence lifetime of MnTCPP.

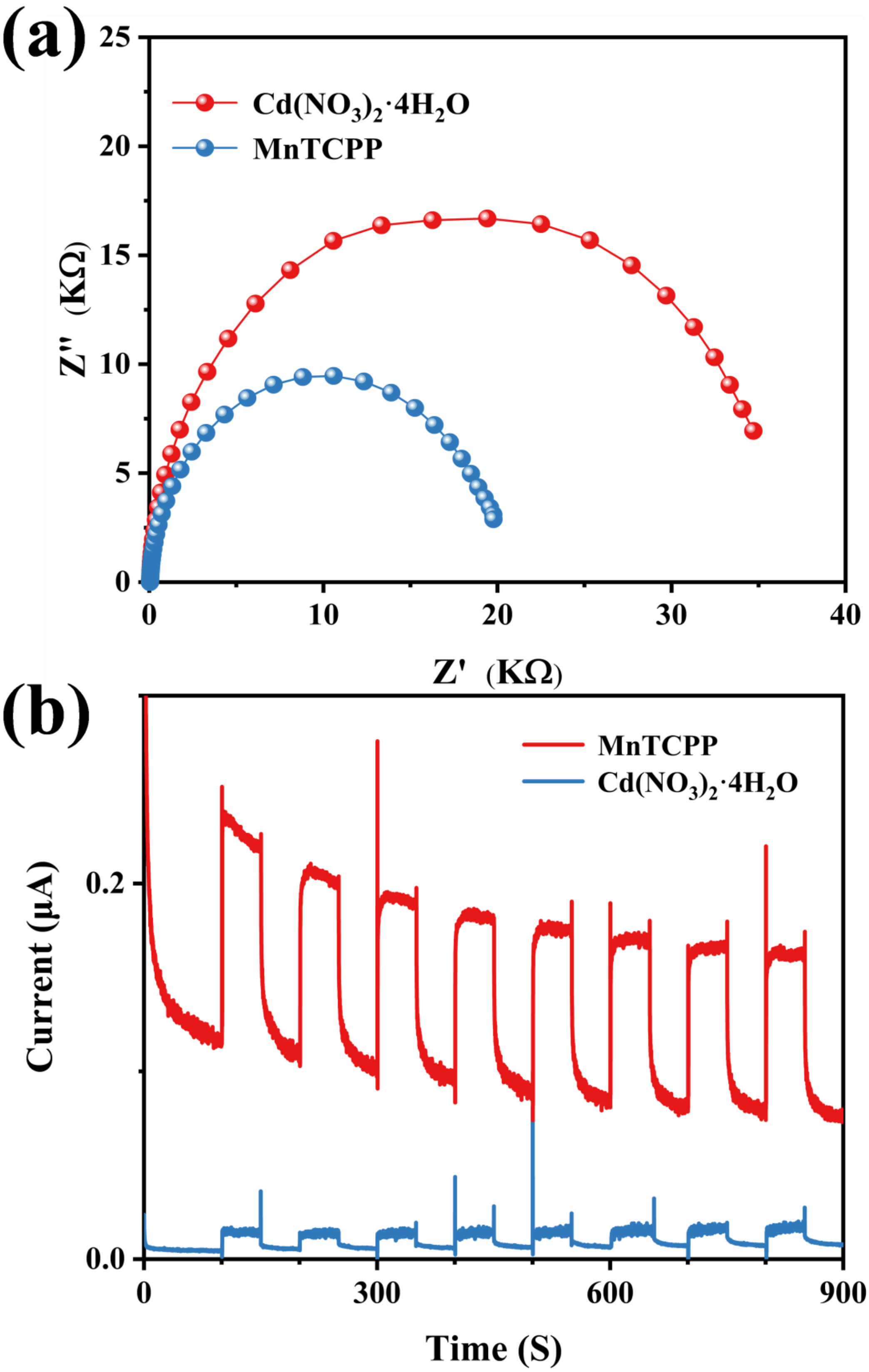

Figure S16. (a) Impedance of MnTCPP and $Cd(NO_3)_2 \cdot 4H_2O$; (b) Photocurrent of MnTCPP and $Cd(NO_3)_2 \cdot 4H_2O$.

Table S2. Comparative Study on the Photocatalytic Oxidation of Toluene to Benzaldehyde under Light Irradiation.

Catalyst	Condition	Yield (%)	Ref.
MnTCPP(Cd)	CH_3CN, 365nm LED, pyridine hydrochloride, O_2, 12h, RT.	85	This
$CdIn_2S_4$-CdS-140	CH_3CN, 420 nm 300 W Xe lamp, O_2, 6h, RT.	80.3	S3
$(PDA)_2AgBiBr_8$	CH_3CN, 300 W Xe lamp, O_2,4h, RT.	64	S4
Fe-PHI/Mn-PHI	H_2SO_4, CH_3CN, 410 nm LED, O_2, 20h/12h, RT.	96/86	S5
CTF-Th-0	Nitromethane, λ>460 nm, O_2, 5h/10h, RT.	84/99	S6

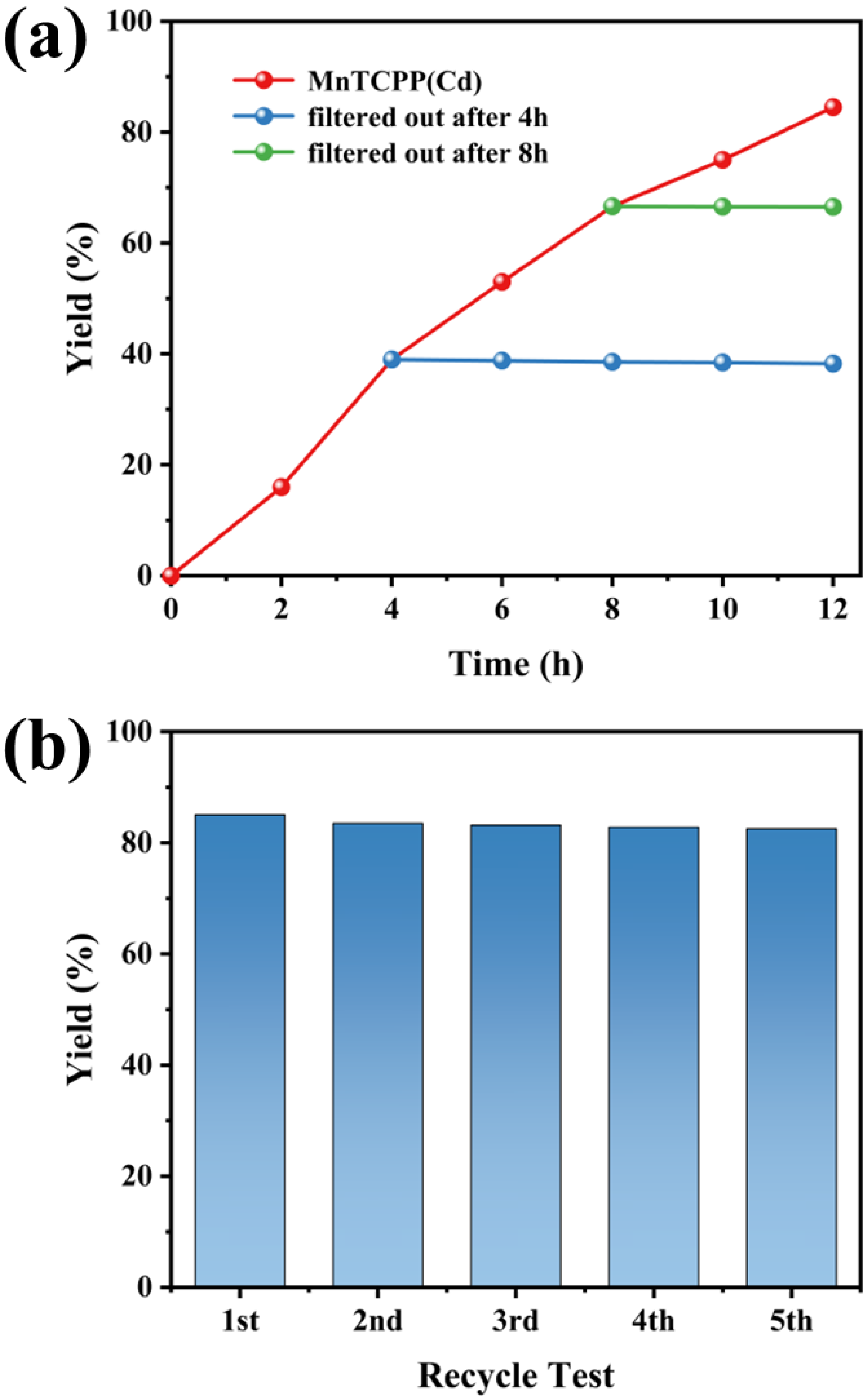

Figure S17. (a) Time-yield tracking of photocatalytic Toluene oxidation (red) and product analysis after catalyst removal (blue and greed); (b) Recycling tests for the photocatalytic oxidation of Toluene.

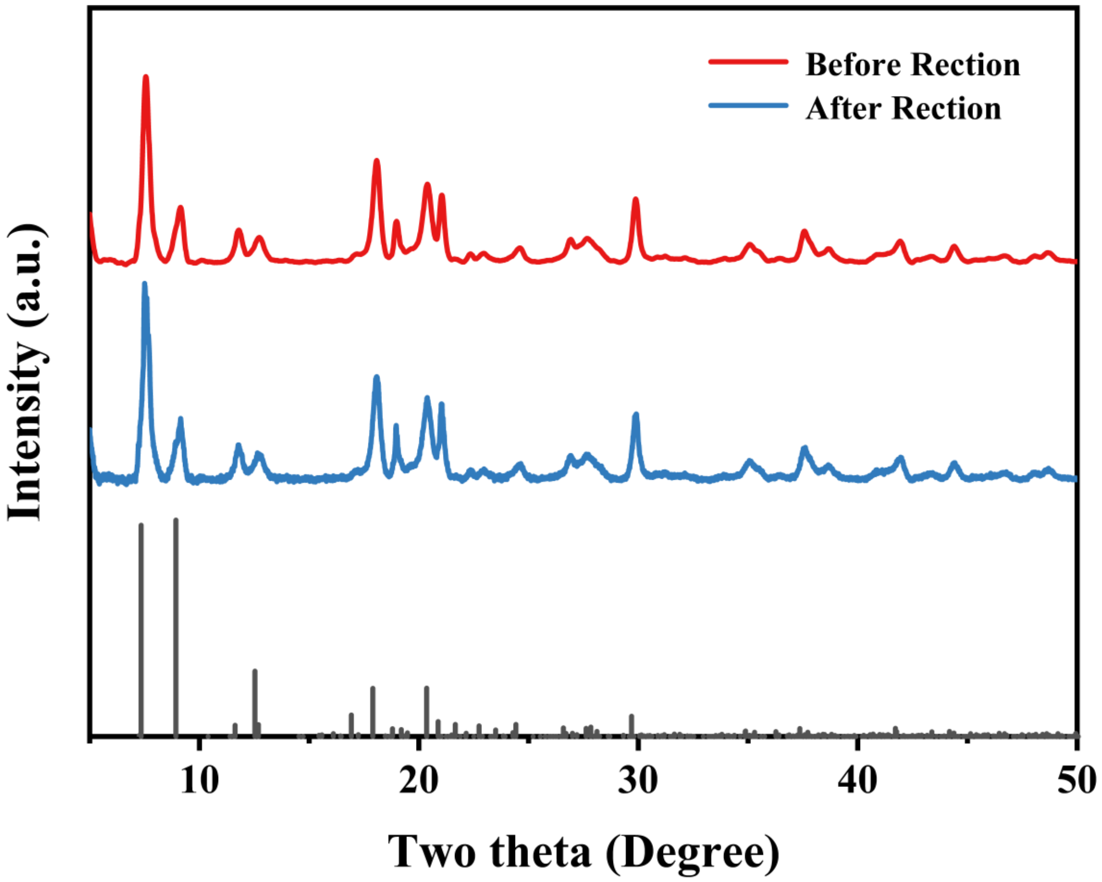

Figure S18. Powder X-ray diffraction patterns of single-crystal simulated MnTCPP(Cd) (black), MnTCPP(Cd) before reaction (red), and MnTCPP(Cd) after reaction (blue).

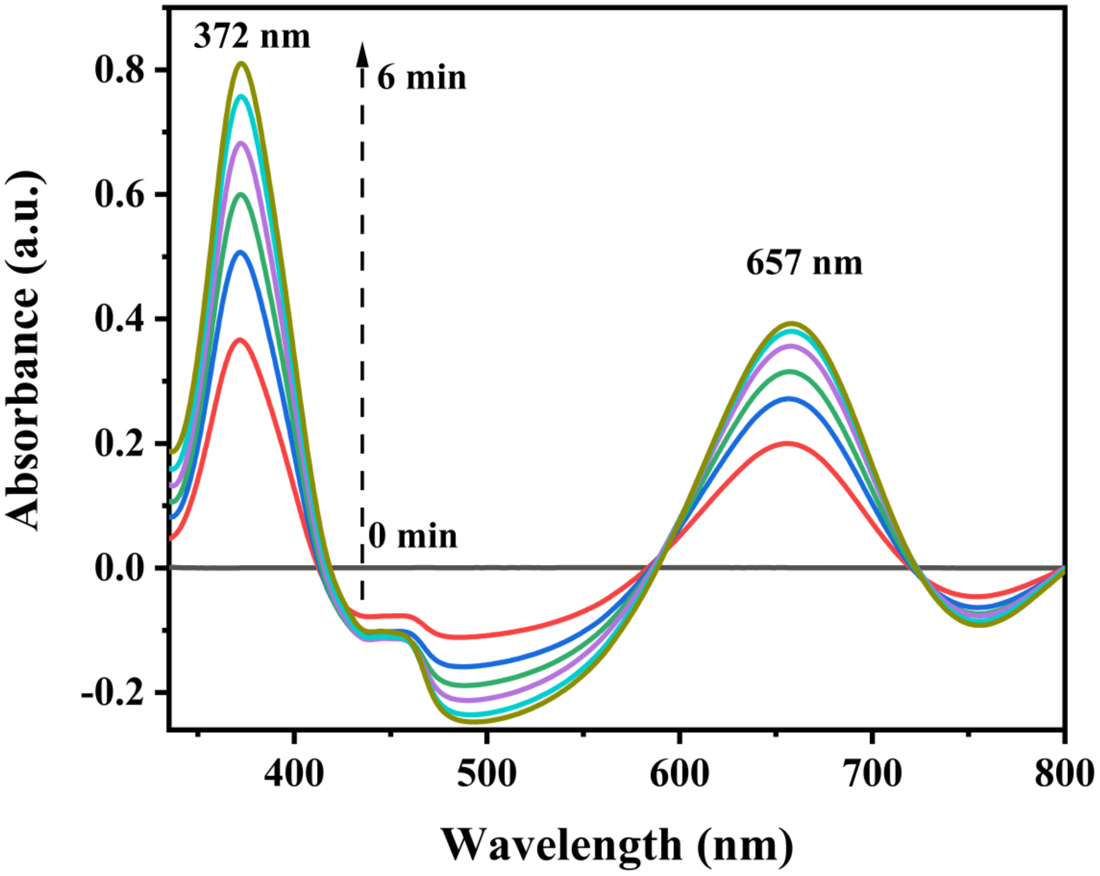

Figure S19. UV-Vis spectrum of FeTCPP(Cd)-catalyzed oxidation of TMB.

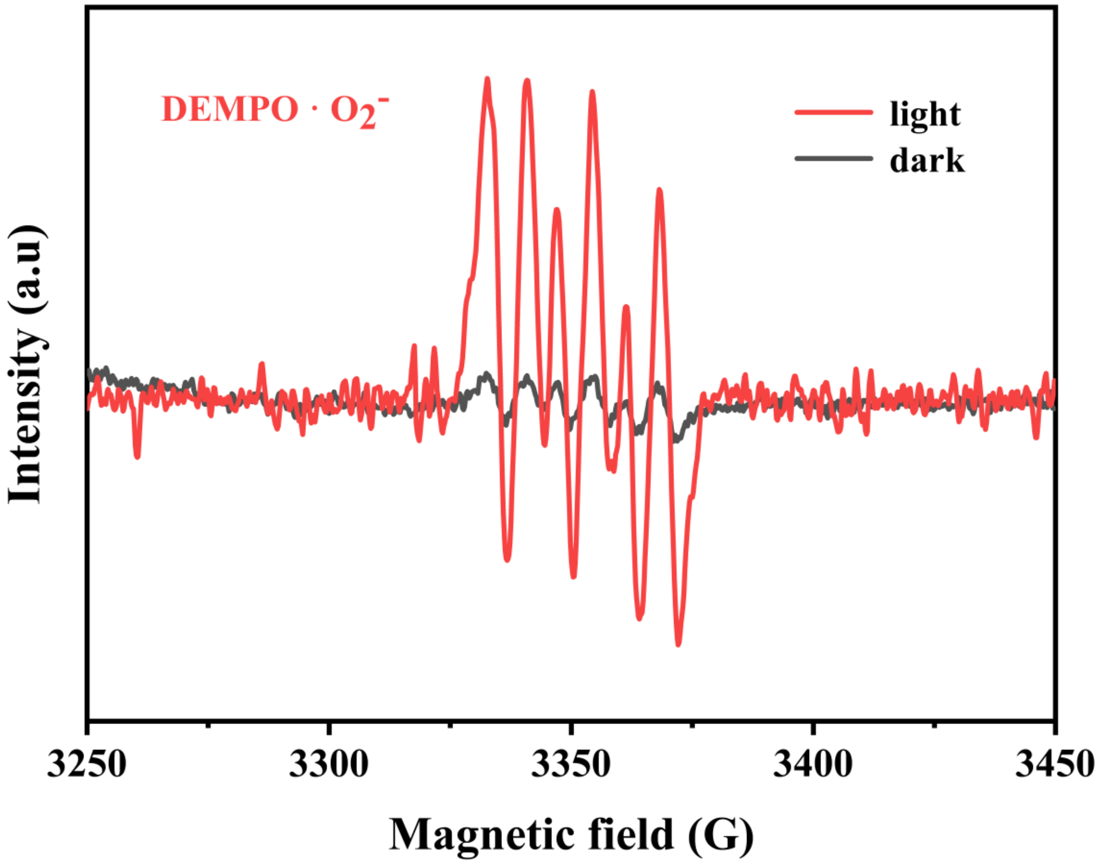

Figure S20. EPR spectra of MnTCPP(Cd) under light irradiation.

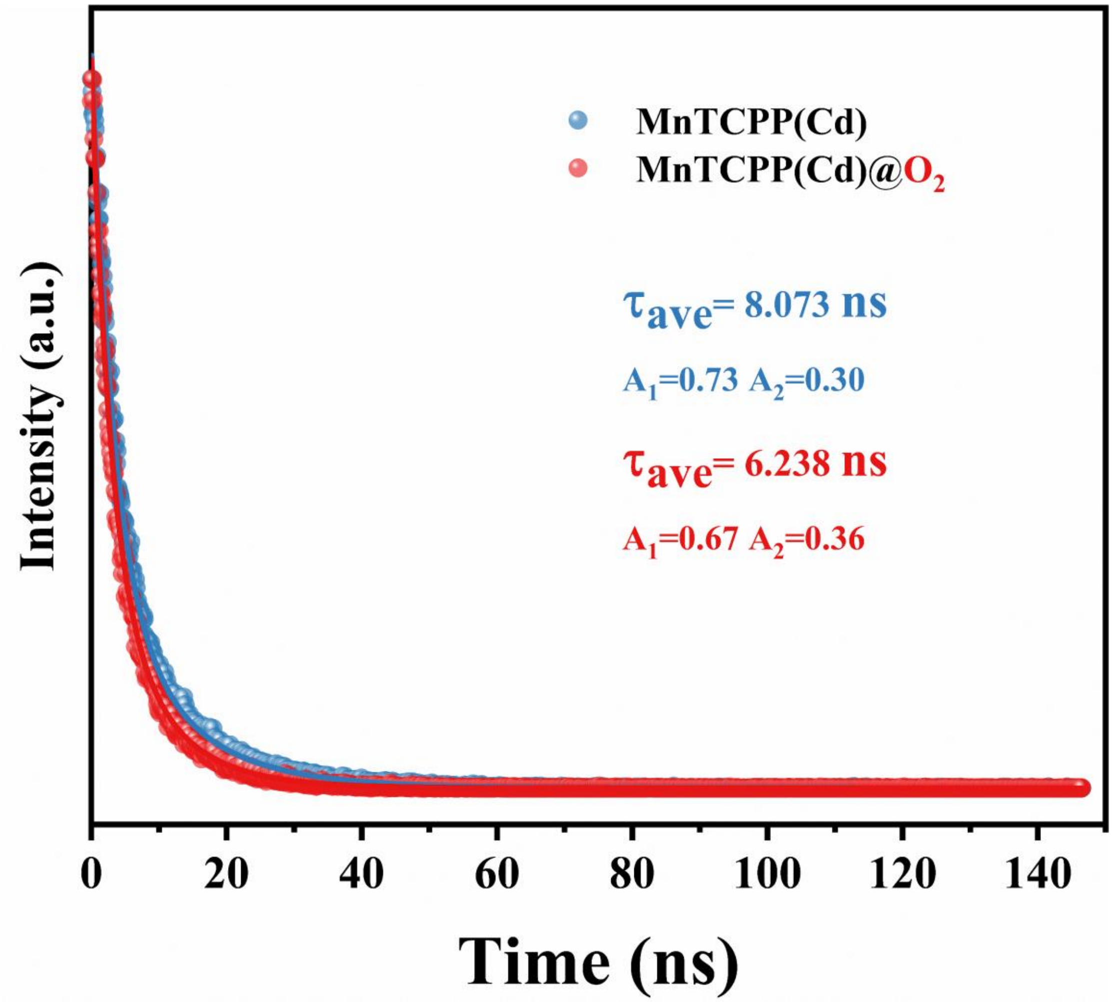

Figure S21. Comparison of fluorescence lifetimes of MnTCPP(Cd) before and after O_2 introduction.

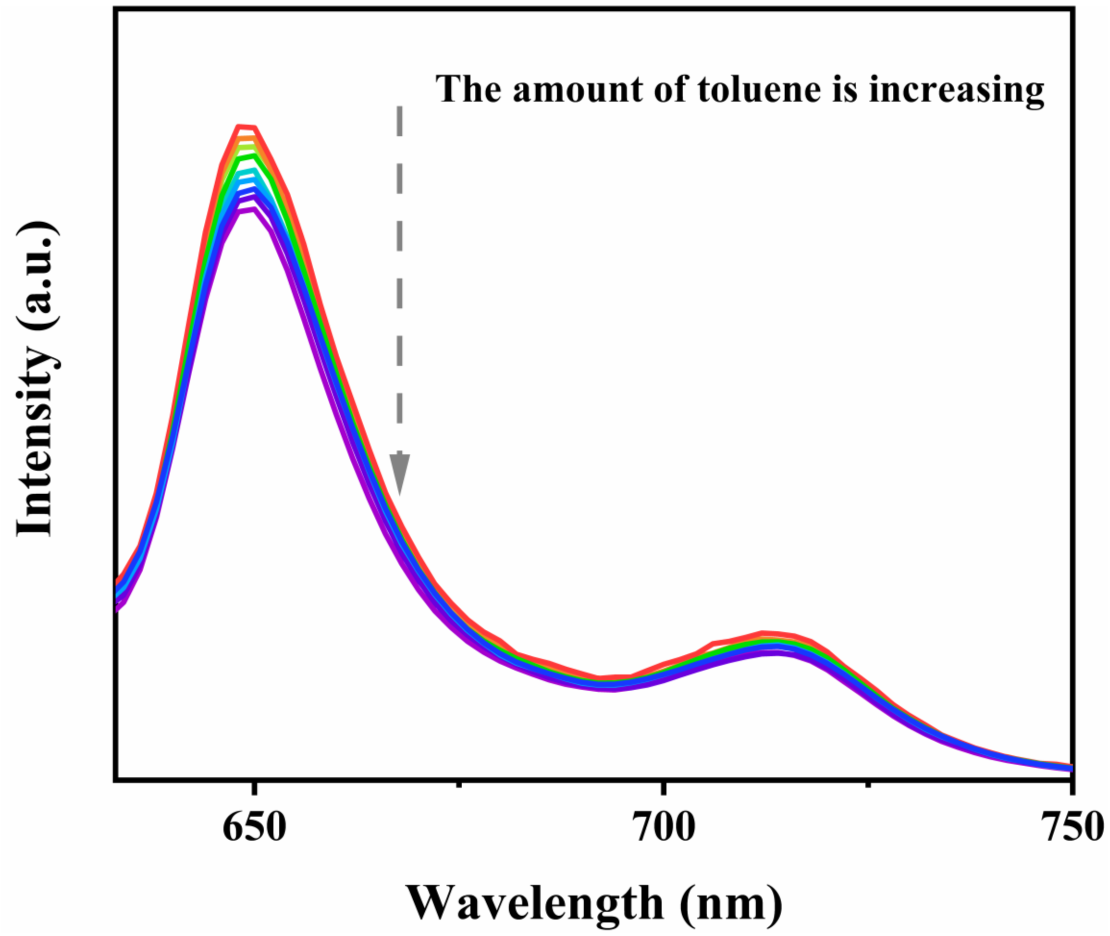

Figure S22. Fluorescence quenching of Toluene by MnTCPP(Cd).

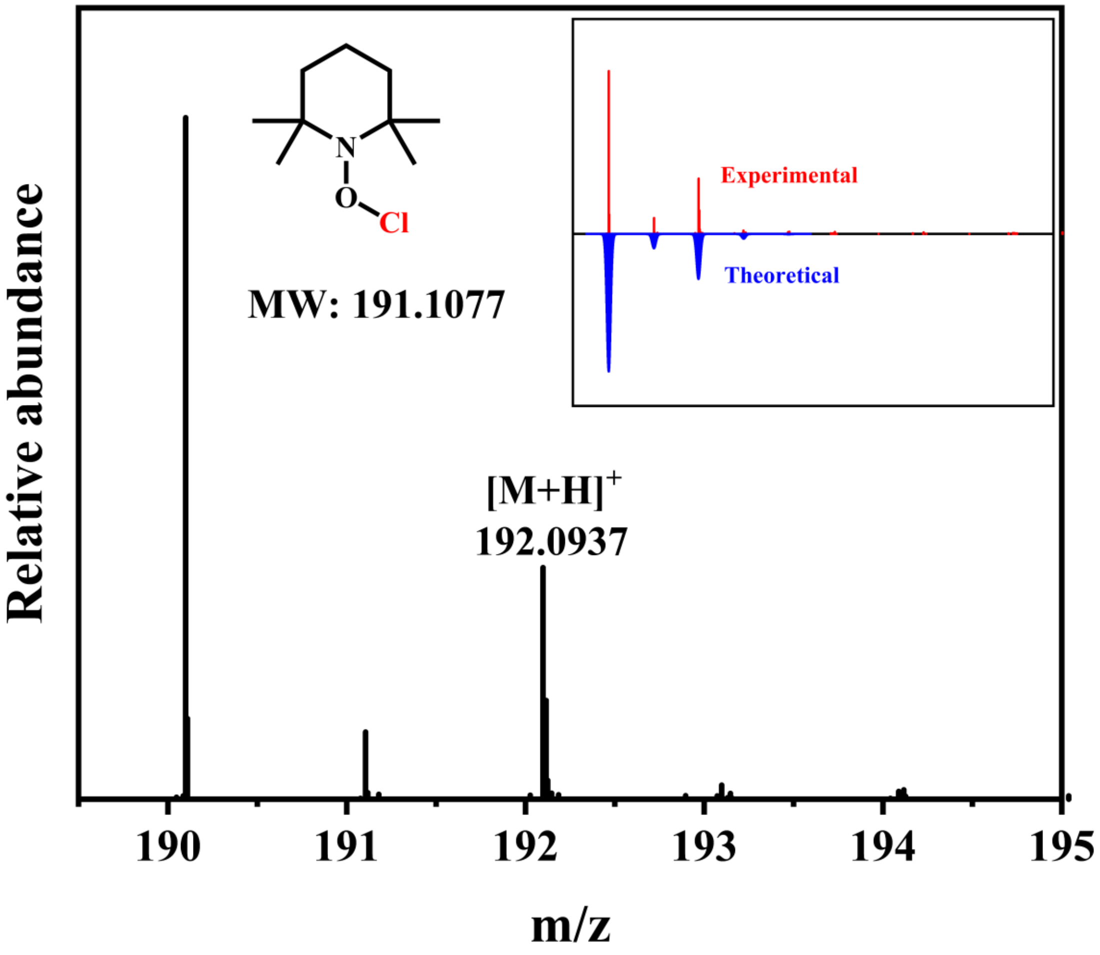

Figure S23. MS for chlorine radical trapping experiment.

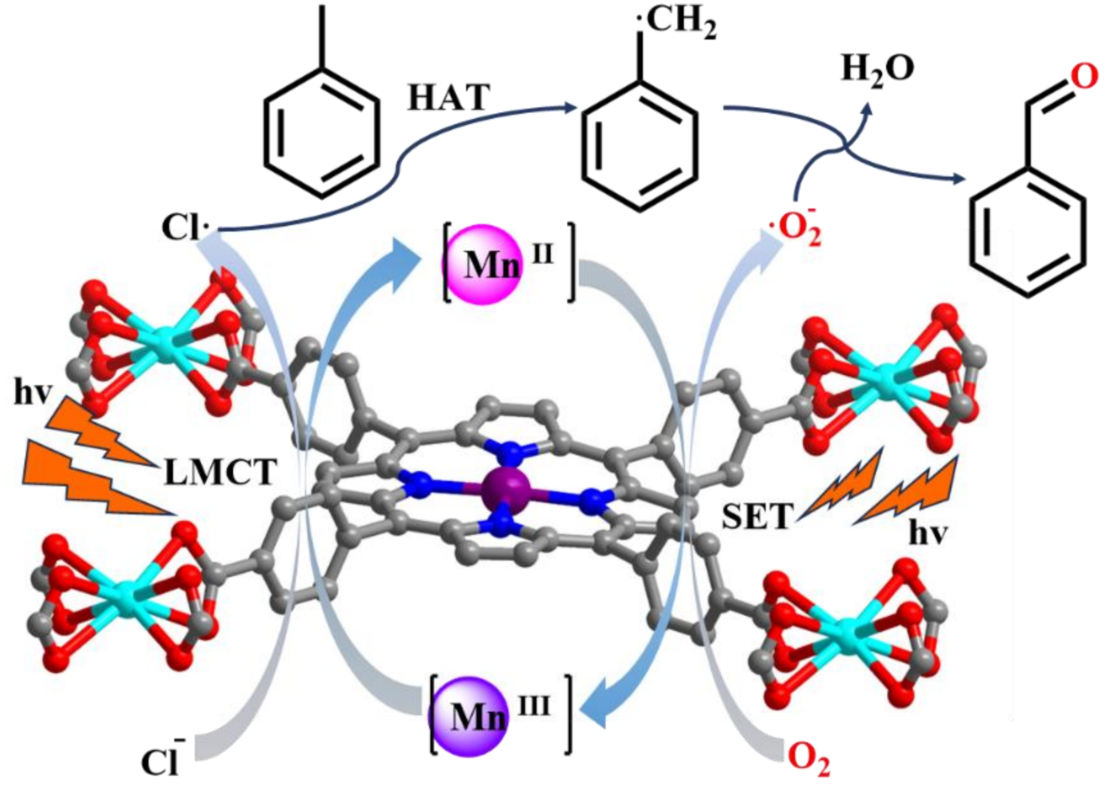

Figure S24. Mechanistic diagram for the photocatalytic oxidation of Toluene by MnTCPP(Cd).

4. ^{1}H NMR Spectra

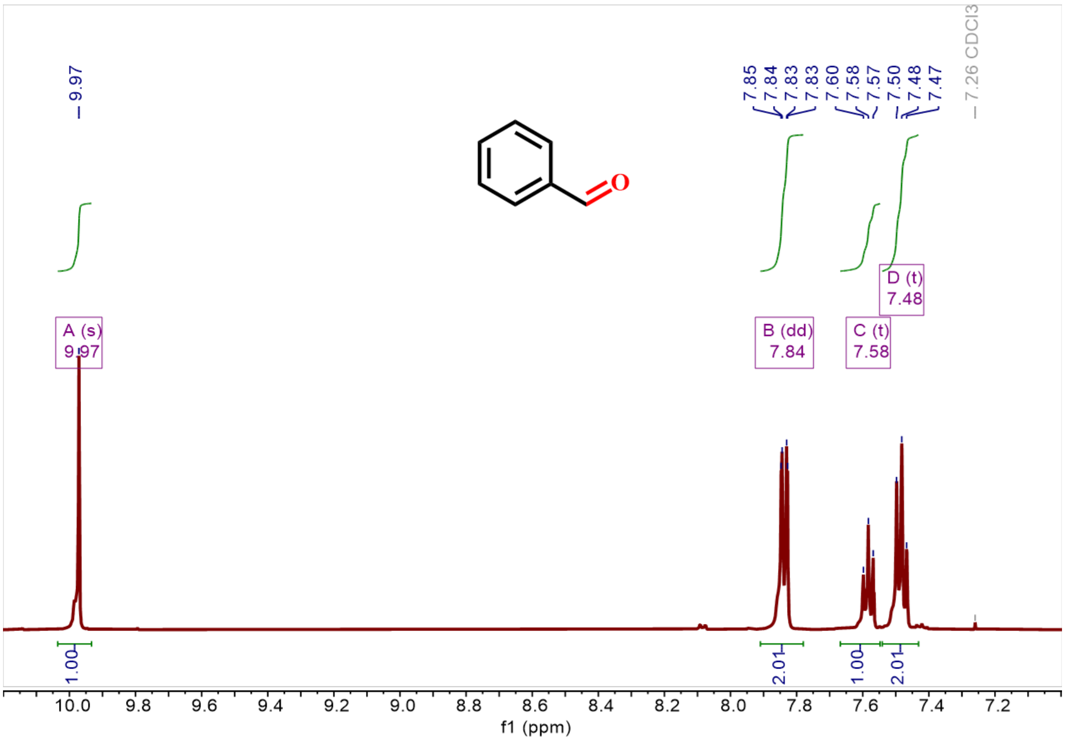

benzaldehyde (1a): ^{1}H NMR (500 MHz, $CDCl_3$) δ 9.97 (s, 1H), 7.84 (dd, *J* = 8.3, 1.4 Hz, 2H), 7.58 (t, *J* = 7.4 Hz, 1H), 7.48 (t, *J* = 7.7 Hz, 2H).

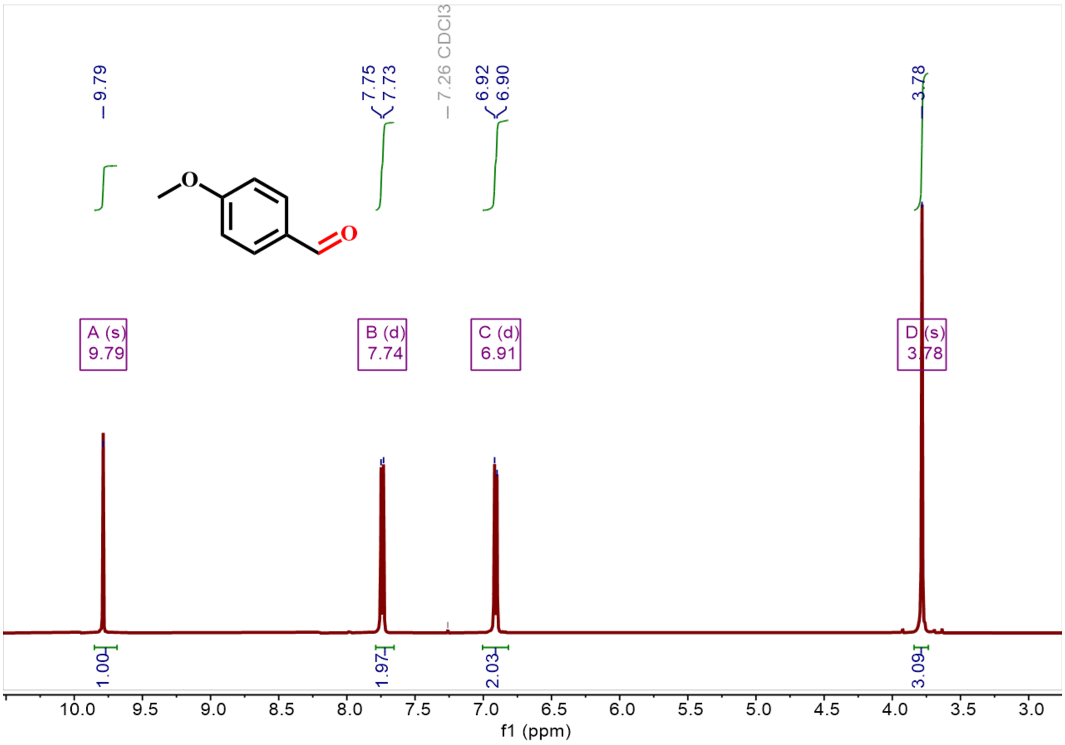

4-methoxybenzaldehyde (1b): ^{1}H NMR (500 MHz, $CDCl_3$) δ 9.79 (s, 1H), 7.74 (d, J = 8.9 Hz, 2H), 6.91 (d, J = 8.9 Hz, 2H), 3.78 (s, 3H).

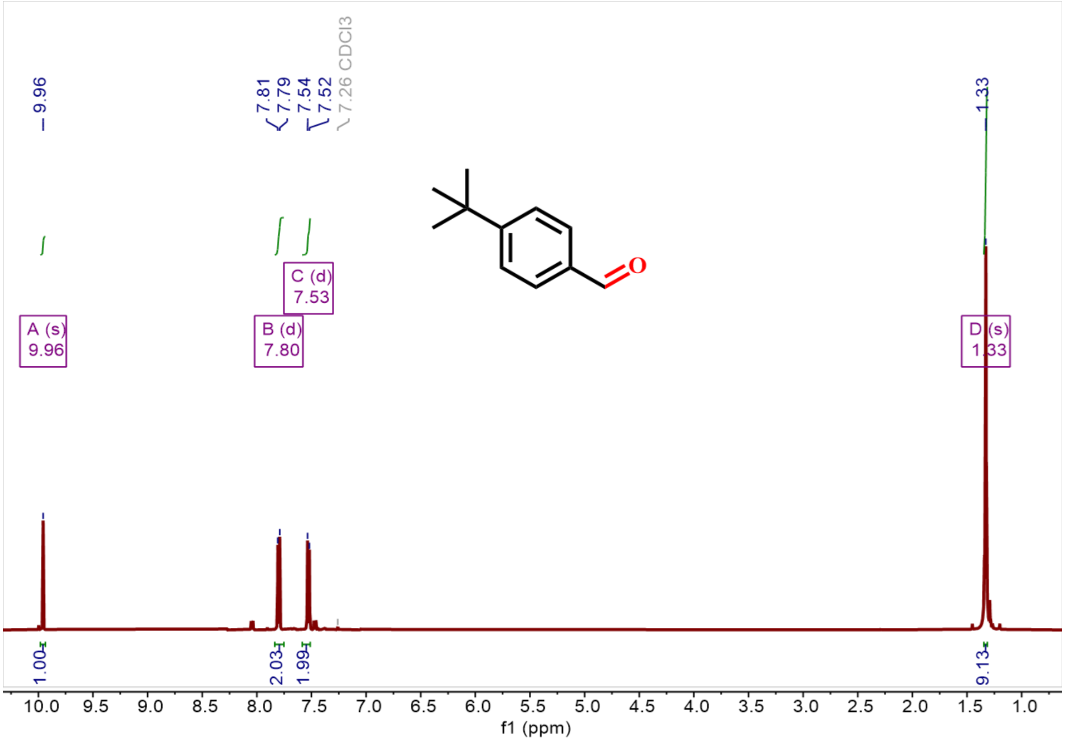

4-tert-Butylbenzaldehyde (1c): ^{1}H NMR (500 MHz, $CDCl_3$) δ 9.96 (s, 1H), 7.80 (d, *J* = 8.7 Hz, 2H), 7.53 (d, *J* = 8.5 Hz, 2H), 1.33 (s, 9H).

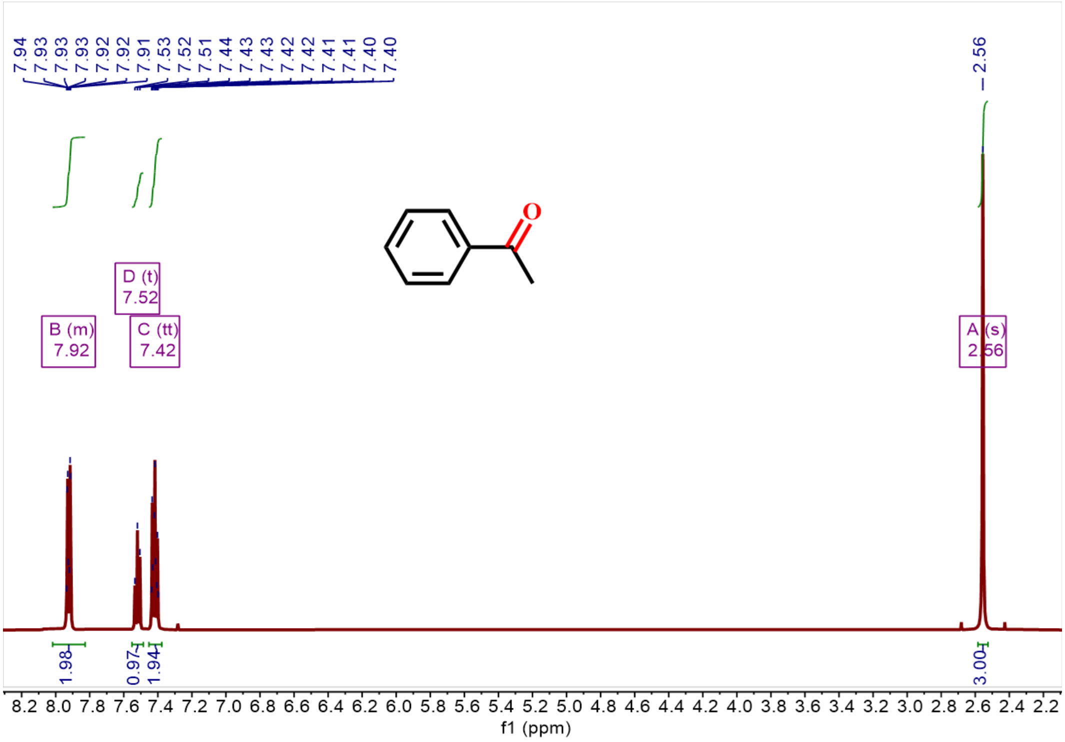

acetophenone (1d): ^{1}H NMR (500 MHz, $CDCl_3$) δ 8.02 – 7.83 (m, 2H), 7.52 (t, *J* = 7.4 Hz, 1H), 7.42 (tt, *J* = 7.5, 1.8 Hz, 2H), 2.56 (s, 3H).

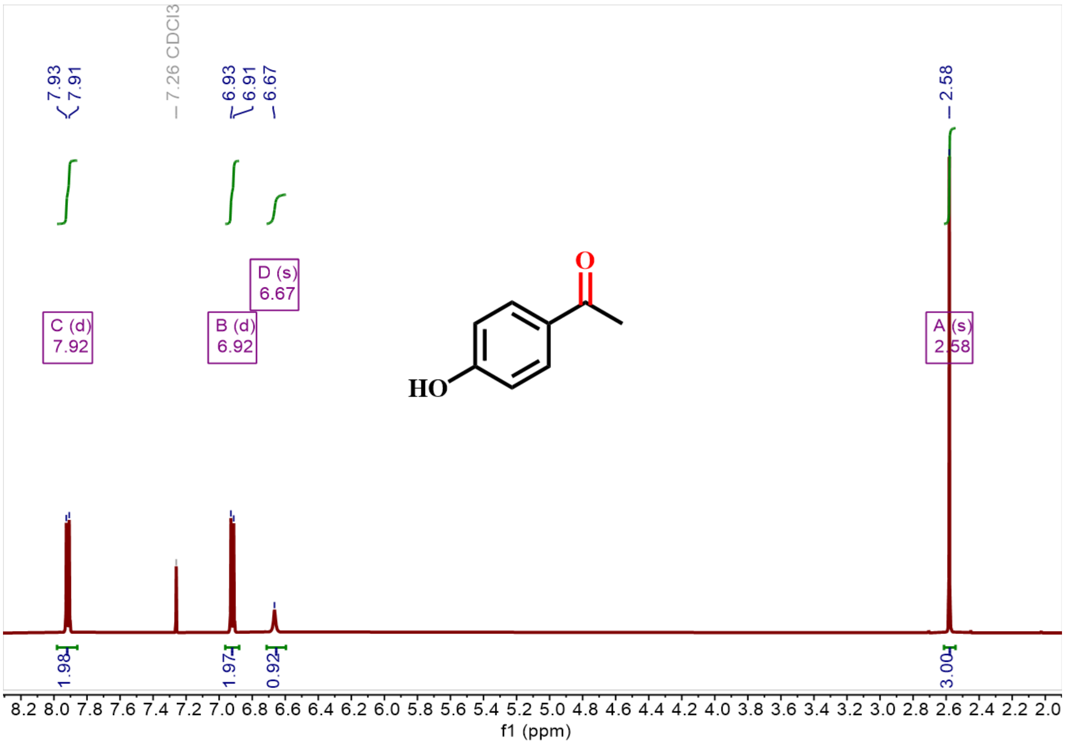

1-(4-hydroxyphenyl)ethan-1-one (1e): ^{1}H NMR (500 MHz, $CDCl_3$) δ 7.92 (d, *J* = 8.9 Hz, 2H), 6.92 (d, *J* = 8.7 Hz, 2H), 6.67 (s, 1H), 2.58 (s, 3H).

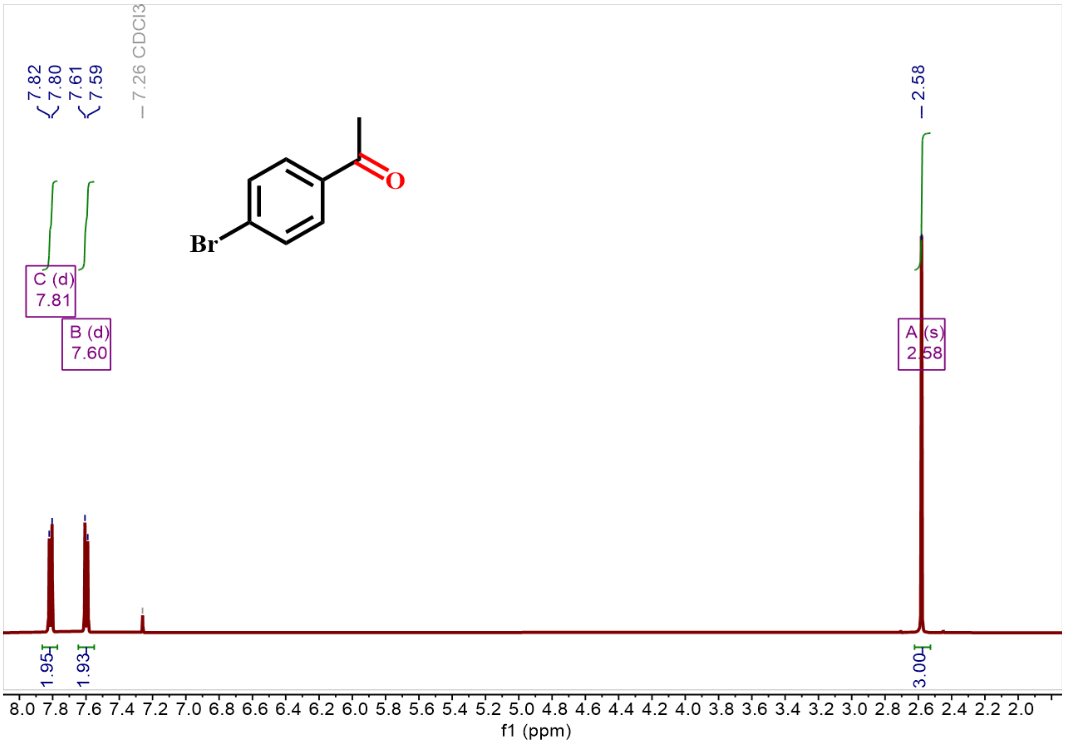

1-(4-bromophenyl)ethan-1-one (1f): ^{1}H NMR (500 MHz, CDCl$_3$) δ 7.81 (d, *J* = 8.5 Hz, 2H), 7.60 (d, *J* = 8.5 Hz, 2H), 2.58 (s, 3H).

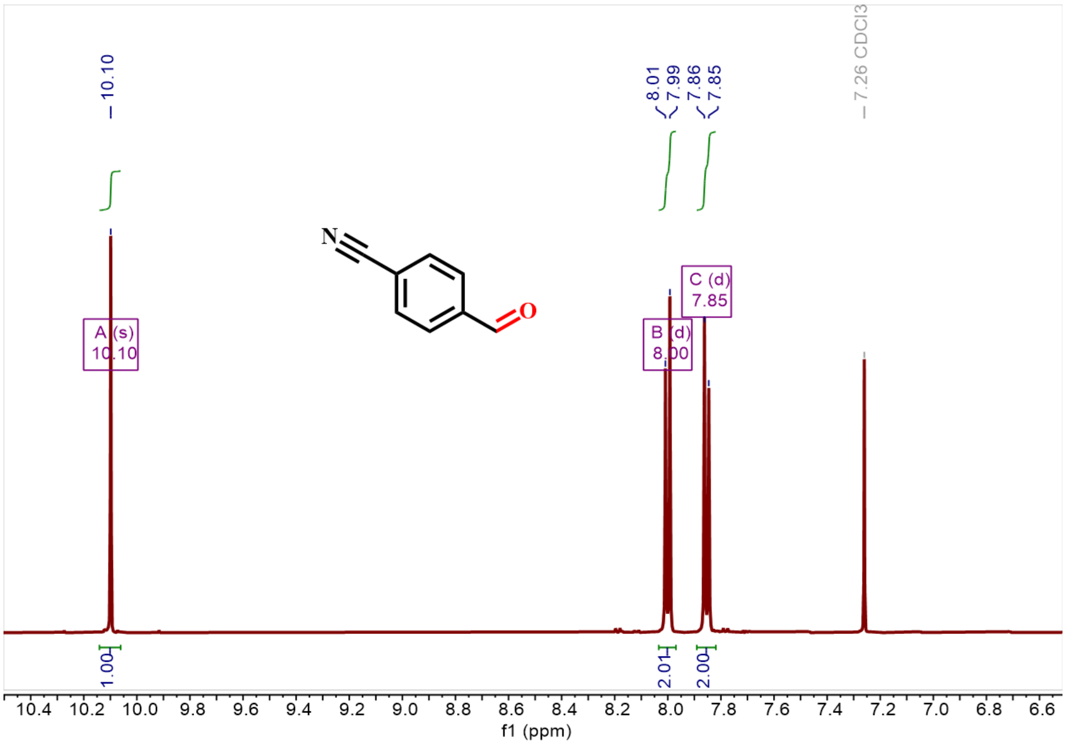

4-formylbenzonitrile (1g): ^{1}H NMR (500 MHz, CDCl$_3$) δ 10.10 (s, 1H), 8.00 (d, *J* = 8.5 Hz, 2H), 7.85 (d, *J* = 8.4 Hz, 2H).

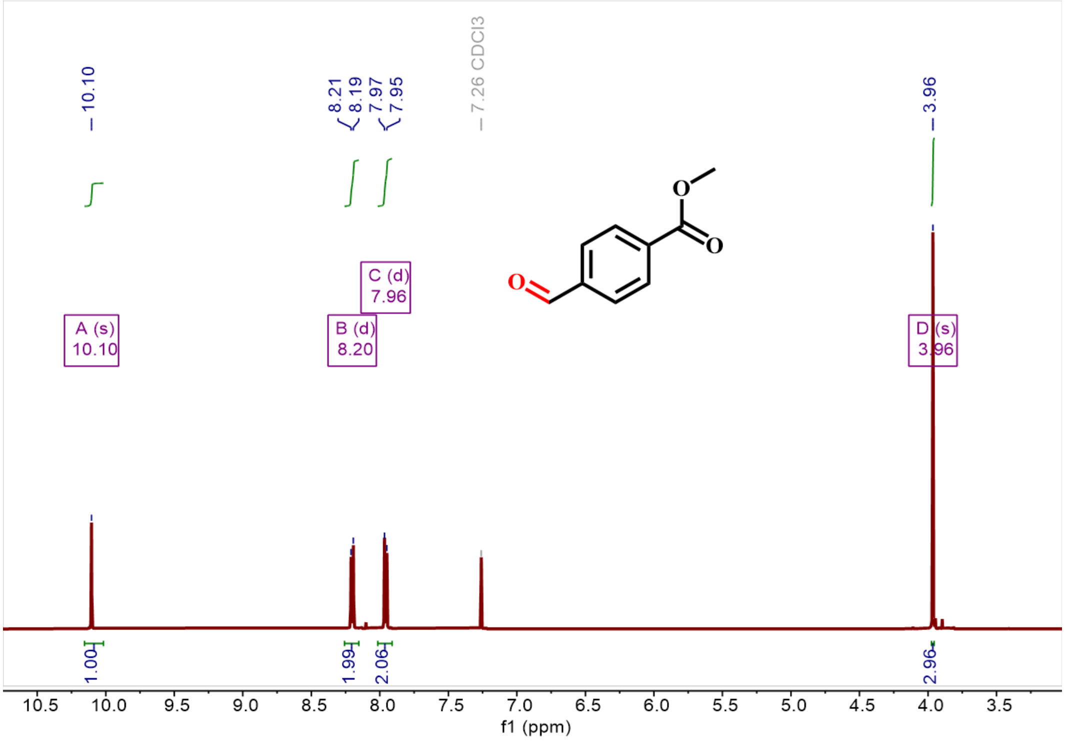

methyl 4-formylbenzoate (1h): ^{1}H NMR (500 MHz, CDCl$_3$) δ 10.10 (s, 1H), 8.20 (d, *J* = 8.2 Hz, 2H), 7.96 (d, *J* = 8.5 Hz, 2H), 3.96 (s, 3H).

References

S1. Y. Wang, L. Zhao, S. Liu, G. Ji, C. He, Y. Tang and C. Duan, *ACS Appl. Mater. Interfaces*, 2023, **15**, 16744–16754.

S2. Z. Zhang, K. Shen, Q. Zhang, C. Duan and X. Jing, *Dalton Trans.*, 2024, **53**, 10060–10064.

S3. Y.-X. Tan, Z.-M. Chai, B.-H. Wang, S. Tian, X.-X. Deng, Z.-J. Bai, L. Chen, S. Shen, J.-K. Guo, M.-Q. Cai, C.-T. Au and S.-F. Yin, *ACS Catal.*, 2021, **11**, 2492–2503.

S4. Z.-J. Bai, J. Xiong, Y. Mao, S. Tian, B.-H. Wang, B. Hu, X. Wang, W. Zhou, C.-T. Au, L. Chen and S.-F. Yin, *Cell Rep. Phys. Sci.*, 2023, **4**, 101591.

S5. M. A. R. da Silva, N. V. Tarakina, J. B. G. Filho, C. S. Cunha, G. F. S. R. Rocha, G. A. A. Diab, R. A. Ando, O. Savateev, I. Agirrezabal-Telleria, I. F. Silva, S. Stolfi, P. Ghigna, M. Fagnoni, D. Ravelli, P. Torelli, L. Braglia and I. F. *Teixeira, Adv. Mater.*, 2023, **35**, 2304152.

S6. S. Li, N. Huber, W. Huang, W. Wei, K. Landfester, C. T. J. Ferguson, Y. Zhao and K. A. I. Zhang, *Angew. Chem. Int. Ed.*, 2024, **63**, e202400101.